The Aeronautical Journal (2022), 1–31
doi:10.1017/aer.2022.20

REGULAR PAPER

The potential impact of adverse aircraft-pilot couplings on the safety of tilt-rotor operations

G. D. Padfield[1,*] and L. Lu[2]

[1]Emeritus Professor of Aerospace Engineering, The University of Liverpool, Liverpool, UK and [2]Senior Lecturer, Cranfield University, UK
*Corresponding author. Email: padfield@liverpool.ac.uk

Received: 12 October 2021; **Revised:** 21 December 2021; **Accepted:** 24 January 2022

Keywords: Aircraft-pilot couplings; Tiltrotor safety; Stability; Handling qualities

Abstract

This paper addresses the potential impact of adverse aircraft-pilot couplings on tiltrotor safety, when a pilot or autopilot attempts to constrain flight dynamics with strong control. The work builds on previously published research on the theory and application of constrained flight to fixed- and rotary-wing aircraft. Tiltrotor aircraft feature characteristics from both types of aircraft and how these determine behaviour in a unique manner is investigated using a FLIGHTLAB simulation model of the XV-15 aircraft. Two different scenarios are explored in detail, using linearised models that reflect the flight-physics of stability for small deviations from trim. First, the control of vertical flight path with longitudinal cyclic pitch and elevator, and the consequences for the stability of the aircraft surge mode and short-period pitch-heave mode. The classical surge-mode instability for flight at speeds below minimum power is shown to apply to the tiltrotor in helicopter mode but alleviated in conversion and airplane modes. The impact on the short–period mode is seen to be a trade-off between the stabilising pitch attitude and destabilising incidence (angle-of-attack) contributions to the flight-path angle. The second example concerns strong control of roll attitude in the presence of adverse aileron-yaw. Here, the yaw-sway motion can be driven unstable, a problem encountered on fixed-wing aircraft with weak weathercock stability, but rare in the rotorcraft world. For both examples, the loss of stability is expressed as the change in sign of effective damping or stiffness stability derivatives. The explanatory theory for these non-oscillatory or low-frequency aircraft-pilot couplings is presented, along with interpretations in terms of handling qualities criteria. The paper also addresses the question of how to translate the findings into a form of aeronautical knowledge useful for the pilot training community.

Nomenclature

A, B, C	coefficients in characteristic equation
$\boldsymbol{A}$, $\boldsymbol{B}$	state and control matrices in the state-space dynamic equations
C_D, C_L	drag and lift coefficients
g	acceleration due to gravity [ft/s^2, m/s^2]
k_1	interlink parameter between DCP and aileron [deg/deg]
k_{w0}	feedback gain from vertical speed to controls [inch (deg)/(ft/min), inch (deg)/(m/s)]
$k_{\dot{w}0}$	feedback gain from vertical acceleration to controls [inch/(m/s^2)]
k_ϕ	feedback gain from roll attitude ϕ to aileron [deg/deg]
L_v, M_q, *etc.*	moment stability derivatives normalised by moments of inertia [rad/(s·ft), 1/s etc.]
L_{X_a}, M_{X_b}, *etc.*	moment control derivatives normalised by moments of inertia [rad/(s^2·inch) etc.]
L_{η_a}, L_{η_r}	roll control derivatives normalised by moments of inertia [rad/(s^2·rad)]
N_{η_a}, N_{η_r}	yaw control derivatives normalised by moments of inertia [rad/(s^2·rad)]
t_D	time to double amplitude [s]
$\boldsymbol{u}$	control input vector
p, q, r	angular velocity components of rotorcraft about fuselage x-, y-, z-axes [deg/s, rad/s]

u, v, w	translational velocity components of rotorcraft along fuselage x-, y-, z-axes [ft/s, m/s]
U_e, W_e	components of trim velocity along aircraft x-axis and z-axis
V_g	horizontal gust [ft/s, m/s]
w_0	vertical velocity [ft/s, m/s]
$\boldsymbol{x}$	state variable vector
X_b, X_c	pilot longitudinal cyclic and collective inputs [inch]
X_{X_b}, Z_{X_b}, *etc.*	force control derivatives normalised by aircraft mass [ft/(s^2·inch) etc.]
X_u, Z_w, *etc.*	force stability derivatives normalised by aircraft mass [1/s, ft/(s·rad) etc.]
α	angle-of-attack [rad]
B_1, θ_{1s}	longitudinal cyclic pitch [rad, deg]
γ	flight path angle [rad]
δ_e,η_e	elevator deflection angle [rad, deg]
η_a, η_r	aileron and rudder deflection angles [rad, deg]
θ, ϕ	Euler pitch and roll angles [rad, deg]
θ_{0D}	differential (proprotor) collective pitch (DCP) [rad, deg]
λ_s	surge mode eigenvalue [-]

Subscript

e	equilibrium or trim
$_{eff}$	effective

Acronyms

6dof	six Degrees of Freedom
APC	Aircraft-Pilot-Coupling
ASRA	Advanced Systems Research Aircraft
DCP	Differential (proprotor) Collective Pitch
FCS	Flight Control System
HQ	Handling Qualities
LCDP	Lateral Control Divergence Parameter
LOC-I	Loss-Of-Control In-flight
PBL	Problem-Based-Learning
PIO	Pilot-Induced/Involved-Oscillation
PVS	Pilot-Vehicle System

1.0 Introduction

The description of Aircraft-Pilot Couplings (APCs) from [1] is adopted in this paper.

> *"Unfavorable aircraft-pilot coupling (APC) events are rare, unexpected, and unintended excursions in aircraft attitude and flight path caused by anomalous interactions between the aircraft and the pilot. The temporal pattern of these pilot-vehicle system (PVS) excursions can be oscillatory or divergent (non- oscillatory). The pilot's interactions with the aircraft can form either a closed-loop or open-loop system, depending on whether or not the pilot's responses are tightly coupled to the aircraft response. When the dynamics of the aircraft (including the flight control system [FCS]) and the dynamics of the pilot combine to produce an unstable PVS, the result is called an APC event.*"

Reference [1] examines a wide range of APC events experienced on prototype and operational aircraft, with a strong emphasis on pilot-induced/involved oscillations (PIOs). In [2], the authors specifically address PIOs, emphasising the importance of a clear definition; so, we have, the *'PIO is a sustained or uncontrollable unintentional oscillation in which the airplane attitude, angular rate, normal acceleration, or other quantity derived from these states, is approximately 180 deg out of phase with the pilot's control inputs, and in which the amplitude of pilot control inputs, aircraft response, or both, is large*

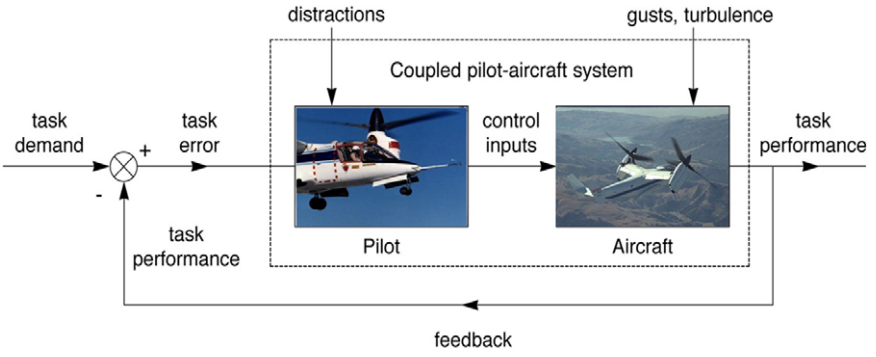

Figure 1. *The coupled pilot vehicle system.*

enough to be intrusive on normal flying.' The emphasis in both [1] and [2] is examination of situations where the control by a pilot can drive the motion being controlled unstable. In the case of rotorcraft, experience has brought a broader perspective. For example, in [3], several cases are cited where it is the interaction of the pilot controlling the aircraft with uncontrolled higher-order dynamics that lead to adverse APCs. Reference [4] presents the example of the interactions of the fuselage and rotor dynamics, examining the physics involved in the energy flow through rotor lead-lag, flap and fuselage attitude dynamics; how negative flow can cause instability and air-resonance behaviour.

In the present paper, we examine a different form of APC, where subtle and insidious nature can lead to quite remarkable, and sometimes difficult for pilots to predict, flight behaviour. A common characteristic is a pilot applying strong control to constrain flight path or aircraft attitude, with the result that the more weakly controlled flight dynamics are driven unstable. These non-oscillatory or low-frequency forms of APC are subtle because pilot attention is on the strongly controlled dynamic, and insidious because they often grow from a slow divergence.

Figure 1 illustrates the coupled PVS, suppressing task errors in the presence of disturbances and distractions. Although handling qualities (HQ) deficiencies make it more difficult to achieve the required suppression, a pilot can normally overcome moderately objectionable (Level 2) deficiencies by increasing compensation. However, with what can be described as hidden deficiencies within the closed loop of the PVS, pilot action can degrade stability and, because attention is on fixing one problem, the emerging APC can develop unseen.

When considering the application to tiltrotor aircraft, two general questions arise from this overview:

a) what characteristics of the aircraft, pilot behaviour or task increase the risk of an APC event?

b) what scope is there for theory to describe and predict the behaviour of the PVS in the presence of an adverse APC?

The first author reported the problem of the loss of speed stability under flight-path constraint for rotary- and fixed-wing aircraft in [5] and [6], citing several fatal accidents where this form of control was a major causal factor; the pilot or FCS attempting to control flight path with cyclic or elevator when flying below the minimum power speed. A flight-physics interpretation is that speed instability occurs because the effective drag derivative, X_{ueff}, changes sign at the minimum power speed. Below this speed, attempts to correct flight-path errors with cyclic or elevator result in the aircraft being pulled or pushed along the constrained flight path by a reversed (effective) drag force. Another consequence of strong flight-path control is loss of stability of the pitch short-period mode, due to the effective vertical damping Z_{weff} and static stability M_{ueff} reversing signs. Less well understood is the problem of the loss of directional stability under bank angle constraint, a handling qualities deficiency that emerged during the early developments of swept-wing aircraft [7]. The problem here relates to adverse aileron-yaw, leading to a reversal in sign of the effective directional stability, N_{veff}. In both cases, strong control by the pilot

dramatically changes the low-frequency dynamics of the PVS, captured in the limit by the distortion of stability derivatives.

These problems are not new; nor are the understandings of the underlying aeronautical physics. Neumark [8] and Pinsker [7] developed theories for the basic physics behind the couplings more than 50 years ago. The first author, with his project supervisor, developed these basics into an APC theory applied to both flight path and attitude control, as described in [9]. Despite the obvious importance of these historical perspectives, accidents continue to occur as reported in [5] and [6], where speed instability was described as a forgotten problem. In the official reports [10,11] on two high-profile accidents described in [5], there was no mention of adverse APCs being the primary causal factor. Inappropriate pilot action was cited, but the dangers associated with the pilot adopting specific control strategies, leading to adverse and destabilising couplings, were not addressed.

Our paper presents the theory of flight stability under constraints and its application to tiltrotor aircraft, using a FLIGHTLAB XV-15 simulation [5]. Specifically, vertical flight-path control in helicopter, conversion and airplane modes for approach configurations are explored in Section 2, to illustrate the risks associated with the loss of speed and short-period mode stability. Roll control in airplane mode is explored in Section 3, to illustrate the potential loss of horizontal flight path and yaw stability. The theory underlying these forms of APC is summarised in Appendix A. Appendix B contains details of the stability and control derivatives derived from the simulation model (FXV-15) in helicopter (H), conversion (C) and airplane (A) modes used in the analysis.

Loss of stability under dynamic constraints can occur well within the normal flight envelope and, as discussed in [1], can be classed as a handling qualities deficiency of the coupled PVS. In [6], the first author made the point that pilot training related to these adverse couplings appears to be inadequate to prepare them for the risks and consequent dangers of entering such flight regimes. How to address this aspect without obscuring the problem with mathematical detail is a challenge that the authors begin to address in Section 4, to bridge the divide between complex flight physics and aeronautical knowledge for aircrew. Specific recommendations for how this might be achieved and expressed in terms of risk and safety margins are presented. The paper is closed with conclusions and recommendations in Section 5.

2.0 Flight-path control and speed stability

2.1 The general problem

In [12], the authors applied the approximation theory for strong flight-path control with cyclic to helicopters, including results from comparative flight and simulation trials with the National Research Council of Canada's Bell 412 (ASRA) and Liverpool's HELIFLIGHT-R simulator, configured with a simulation of ASRA. The results confirmed the predicted loss of stability through the adverse coupling. Figure 2 shows an example result from the trials. From an initial trim speed of 50kts, a disturbance was simulated with a pulse input in cyclic. The pilot's task was then to maintain the aircraft's flight path (rate of descent), initially using both cyclic and collective, then with only cyclic. The trajectories in Fig. 2 show that the pilot maintained airspeed within 5kts using the coupled-control technique. With cyclic-only control, the airspeed gradually reduced, decelerating to the hover in the simulator; in flight the pilot recovered when the airspeed reached 20kts. Pilots are taught to use the coupled technique when flying below minimum power speed, or, if assisted by an autopilot, to engage both airspeed and vertical speed hold modes.

In 2013, three years after this research was first published, there were two accidents caused by such couplings; a Boeing 777 on approach to San Francisco [10] and a Eurocopter AS-332 on approach to Sumburgh [11]. The first author discussed these accidents in detail in [5], drawing attention to the apparent lack of awareness of pilots and their training organisations concerning the true nature of the problem.

An aircraft is naturally stable when flying below minimum power, exchanging potential and kinetic energy in the phugoid, but speed stability is threatened by inappropriate pilot control action, as in the case

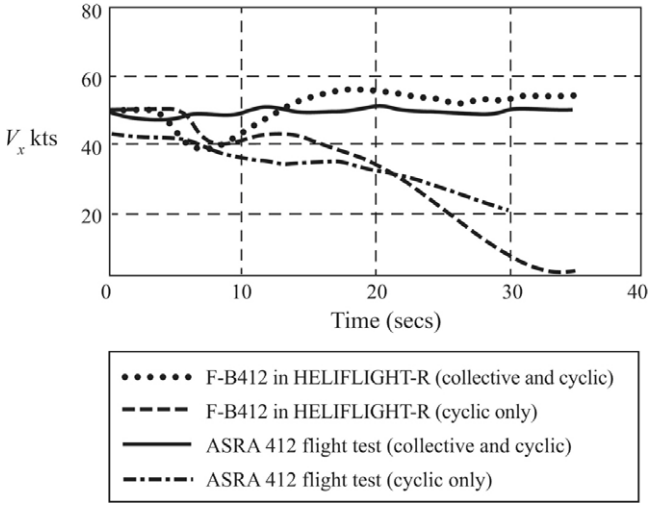

Figure 2. *Variation of flight speed with time during trials with flight-path constraint; comparison of flight and simulator [5,12].*

of the B-777 accident. The same effect can be brought about by automatic control, as in the case of the AS-332 accident, through the functioning of the vertical-speed hold mode of the autopilot. In both scenarios, the aircrew did not monitor the consequent speed reduction and only took recovery action when it was too late to avoid a crash. Such accidents occur all too often, with the initial problem described, misleadingly, as the approach being unstable. The use of the term unstable refers to flight conditions outside defined trim speeds and flight-path angles at specified horizontal and vertical distances from the landing point. This has nothing to do with the aircraft's stability and is a classic example of aeronautical physics being lost in the translation to operational phraseology. The argument that distinguishing between trim and stability is too subtle, or complicated, for aircrew or training organisations has no merit in the authors' opinion. Rather more, aircrew understanding of the physical causes and effects of adverse APCs is considered crucial to elimination of accidents arising from such causal factors. We return to this topic later in the paper, in Section 4, but first the aeronautical physics.

Figure 3 shows the trim power curves for the FXV-15 in H-mode, C-mode and A-mode, with and without rotor-wake on wing interference, in level and descending flight; flight test points from [13] are included, although the precise test conditions for these are not known. The simulated impact of rotor-wake on wing interference is suspected as being too abrupt between 40 and 60kts, and the analysis is restricted to cases where the interference effects are minimal. The shape of the power curves in Fig. 3 reflects a similar pattern for the aircraft drag, albeit with the minimum shifted to a higher velocity. When flying below minimum drag, a reduction in velocity leads to an increase in drag and a further reduction in velocity; seemingly unstable, in contrast to stability for speed perturbations during flight above minimum drag. As will be shown, this intuitive interpretation in terms of stability is incorrect and it is only through the action of closed-loop control that stability is compromised.

Consider the aircraft on an approach, with speed and flight path under the control of a pilot or autopilot system. To analyse stability, we assume the deviant dynamics to be small perturbations about the trim condition, and write the equations of longitudinal (pitch-surge-heave) motion in the linearised form,

$$\frac{\mathrm{d}}{\mathrm{d}t}\begin{bmatrix} u \\ w \\ q \\ \theta \end{bmatrix} - \begin{bmatrix} X_u & X_w & X_q - W_e & -g\cos\Theta_e \\ Z_u & Z_w & Z_q + U_e & g\sin\Theta_e \\ M_u & M_w & M_q & 0 \\ 0 & 0 & 1 & 0 \end{bmatrix} \begin{bmatrix} u \\ w \\ q \\ \theta \end{bmatrix} = \begin{bmatrix} X_{X_b} \\ Z_{X_b} \\ M_{X_b} \\ 0 \end{bmatrix} X_b \tag{1}$$

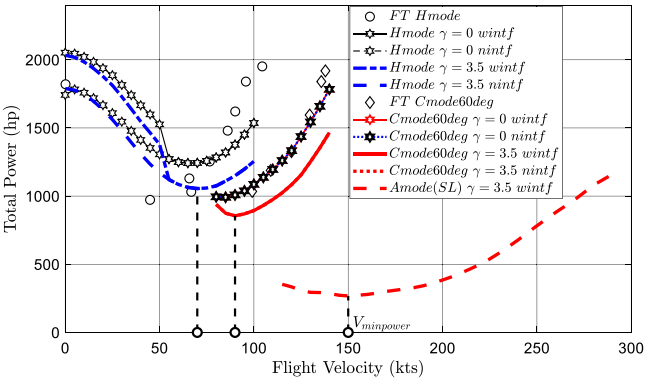

Figure 3. *Power curves for the FXV-15 in various configurations showing minimum power speeds (note predicted C-mode power lines with (wintf) and without (nintf) interference overlie).*

u and w are the deviant surge and heave translational velocities, q and θ are the deviant pitch rate and Euler attitude respectively; U_e and W_e are the equilibrium (trim) velocities and Θ_e the corresponding trim pitch attitude. X_u, M_q etc. are the stability derivatives and X_{Xb}, M_{Xb} etc. are the control derivatives for the pilot's longitudinal stick, X_b. The pilot also has the collective control lever X_c, for control of flight path and speed, but the present analysis is concerned only with flight-path control with centre stick. For a tiltrotor, the centre stick has a primary function of controlling longitudinal cyclic pitch of the proprotors in H-mode and elevators in A-mode. For the XV-15, the elevator is also connected to X_b in H-mode and C-mode with the same gearing at all nacelle angles. In C-mode, the cyclic pitch control is blended out as a function of nacelle angle such that it is completely phased out in A-mode. In Appendix B, the derivatives for all three controls, the cyclic pitch (B_1 in FLIGHTLAB notation, $-\theta_{1s}$ in the notation of [5]), elevator angle (δ_e in FLIGHTLAB notation, η_e in the notation of [5]) and pilot's stick X_b, are tabulated, along with the stability derivatives. Aft movement of the stick gives positive (up) elevator angle and negative B_1 (proprotor disc tilts back). Appendix B also contains details of the control gearings on the XV-15 aircraft used in the FXV-15.

2.2 Constrained flight-path control in H-mode

The natural pitch-surge-heave stability of the aircraft is quantified in terms of the longitudinal eigenvalues shown in Fig. 4, for the FXV-15 in H-mode from hover to 80kts. The assumption here is that stability is not strongly affected by the couplings with lateral-directional motion, as discussed in [5]. The low-frequency phugoid mode is shown to be stable between 40–80kts with a time to half-amplitude of about 14secs. With a period of about 21secs, the phugoid motions decay to half-amplitude in about two-thirds of a cycle. The civil certification standards for dynamic stability in instrument flight conditions [14] require that *'any oscillations having a period of 20 seconds or more may not achieve double amplitude in less than 20 seconds'*. It is noted that, while the FXV-15 phugoid is stable at speeds above 40kts, instability is allowed according to the CS-29 requirement. The short-period mode morphs from the pitch and heave subsidences between 20–30kts, advancing to an oscillation with a period of about 5secs and time to half amplitude of about 0.5secs at 80kts. At 40kts, the oscillation has higher relative damping, so decaying in a much smaller fraction of the 'short' period than at 80kts. CS-29 requires that *'any oscillation having a period of less than 5 seconds must damp to half amplitude in not more than 1 cycle'*.

In H-mode, control of flightpath and speed are normally achieved through pilot action with both centre stick and collective, as discussed earlier. In the present study, we are concerned specifically with flight-path control using the centre stick. The behaviour of the aircraft then differs markedly for flight

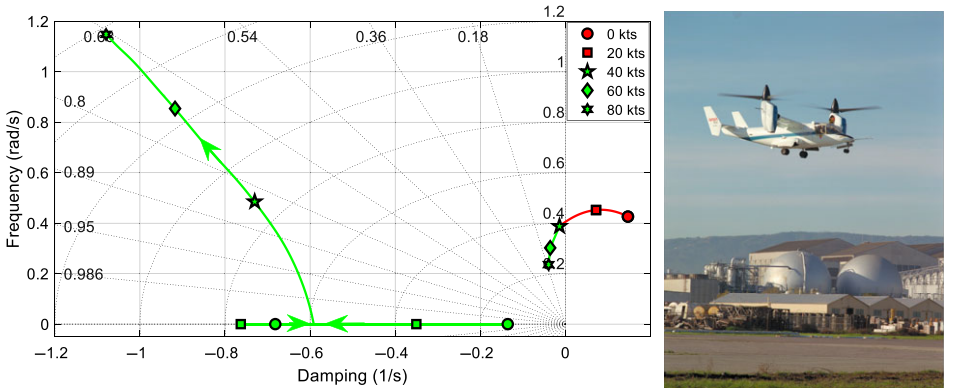

Figure 4. *Longitudinal eigenvalues as a function of speed for the FXV-15 in H-mode; descent $\gamma = 3.5$deg XV-15 in hover (photo NASA).*

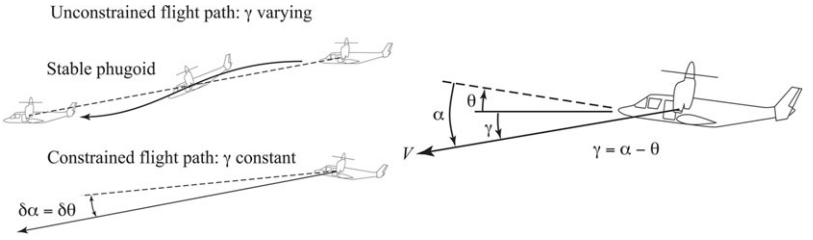

Figure 5. *Flight trajectories following a disturbance with unconstrained and constrained flight path.*

on the front side (above min-power speed) compared with flight on the back side of the power curve. To begin with, we consider the classic case discussed by Neumark in [8], where the flight path is perfectly constrained; the aircraft effectively flying on sky-rails. Figure 5 illustrates the difference between the unconstrained and constrained scenarios.

As shown, the flight-path angle (positive for descent) is the difference between the aircraft incidence and pitch angle.

$$\gamma = \alpha - \theta \tag{2}$$

For unconstrained flight, a pulse-like disturbance in velocity or pitch attitude excites both the short-period and phugoid modes, the former decaying rapidly. The phugoid takes much longer to decay but the aircraft would eventually return to its trim condition on the original flight path. Flying on either the front side or the back side of the power curve (Fig. 3), the transient phugoid involves an exchange of potential and kinetic energy at essentially constant angle of incidence. For the constrained flight-path case, the perturbed incidence and pitch angle are equal, the aircraft remaining on the initial flight-path trajectory. Any disturbance would impact the speed, incidence and pitch, but the loss of speed is not converted into potential energy as in the phugoid; the increasing or decreasing induced drag on the back side of the power curve thus continually slowing or accelerating the aircraft. On the front side of the curve, perturbations in speed are countered by the growing or reducing parasite drag such that the surge motion is stable, even under constrained flight. This physical reasoning can be reinforced by the analytics, as follows.

Assuming small angles of incidence and flight path, we can write the total flight speed $V \approx U_e$, then from Equation (2), on the flight path, the deviant vertical velocity w_0 can be written as,

$$w_0 = w - U_e\theta \tag{3}$$

In the constrained flight-path scenario, $w_0 = 0$ (with zero or non-zero trim value), and w and $U_e\theta$ are locked together as described above. The deviant equations of motion can then be simplified to form the coupled surge and heave dynamics.

$$\begin{aligned} &\frac{du}{dt} - X_u u - \left(X_u - \frac{g}{U_e}\right) w = 0 \\ &-Z_u u - Z_w w = 0 \end{aligned} \tag{4}$$

These equations can be combined into a single surge mode with eigenvalue expressed as an effective drag derivative X_{ueff},

$$\lambda_s = X_{ueff} = X_u - \frac{Z_u}{Z_w}\left[X_w - \frac{g}{U_e}\right] \tag{5}$$

This is Neumark's approximation to the speed mode for fixed-wing aircraft and the analysis in [8] showed that the mode becomes unstable when the slope of the drag vs lift curve is equal to 1.5 times the ratio of drag to lift; this is the condition for minimum power and expressed in coefficient form as,

$$\frac{3C_D}{2C_L} = \frac{\partial C_D}{\partial C_L} \tag{6}$$

From Equation (4), the contribution of the weight component along the flight-path ($g\alpha$) is destabilising and the scaling by the heave derivative ratio (approximately inversely proportional to C_L) determines its impact on speed stability. The X_w effect is typically small for H-mode in low-speed flight, but will be shown to have a major impact on speed stability in C-mode. An important point here concerns the minimum power point as the stability divide. This assumes that the thrust-generating device (e.g. rotor, propeller, turbofan) contributes to the drag derivative X_u [15] through the governed rotorspeed. For the case where there is little or no thrust response to u perturbations (e.g. turbojet-powered aircraft, glider), the stability boundary is located at the minimum drag speed [5]. Aircrew training is often couched in energy management terms for flight above and below minimum drag, and thrust required to trim, with little or no mention of power. The minimum power (maximum endurance) speed is approximately 0.75 of the minimum drag (maximum range) speed.

Both [5] and [12] showed that the approximation to the surge mode as an effective drag derivative (Equation (5)) also applies to helicopters. Figure 6 shows λ_s as a function of speed for the FXV-15 in H-mode, constrained to fly a 3.5deg descending flight-path angle. The mode is predicted to become unstable around 75kts, slightly higher than the minimum power speed in Fig. 3. This simple theory predicts that the surge mode instability is more severe at lower speeds, with time to double amplitude (t_D) reducing to a few seconds at about 30kts. Longitudinal cyclic is totally ineffective at controlling flight path at very low speed; the increasing rotor downwash overpowering the upwash as the rotor disc incidence increases.

The stability divide is shown schematically in Fig. 7. The approximation predicts a response to a horizontal gust V_g being driven by a (normalised) force $\lambda_s V_g$, the effective drag force, that subdues the effect of the disturbance for flight on the front side and increases the effect for flight on the back side of the power curve.

The surge mode discussed above represents the limit of the pilot applying feedback control with cyclic or elevator to maintain constant flight-path angle. This limiting case, effectively locking together incidence and pitch attitude, implies infinite feedback gain and the question arises as to what value of finite gain would be required to drive the surge mode unstable? Once again, the theory for finite gain analysis for helicopters was presented in [5,12], and here we extend its application to tiltrotor aircraft. Based on the power curves in Fig. 3, the flight speeds of 55kts and 75kts are selected for analysis.

The proportional feedback control law takes the form,

$$X_b = k_{w0} w_0 \tag{7}$$

X_b is the longitudinal stick, w_0 the vertical velocity and k_{w0} is the feedback gain. In the following analysis, we examine the three feedback loops: control with B_1, with δ_e and combined with X_b. Recall that $+B_1$

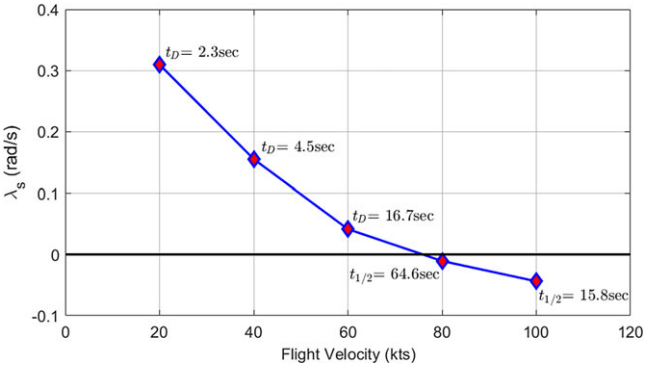

Figure 6. *Approximation to the surge eigenvalue as function of airspeed, FXV-15 H-mode, descent* $\gamma = 3.5deg$.

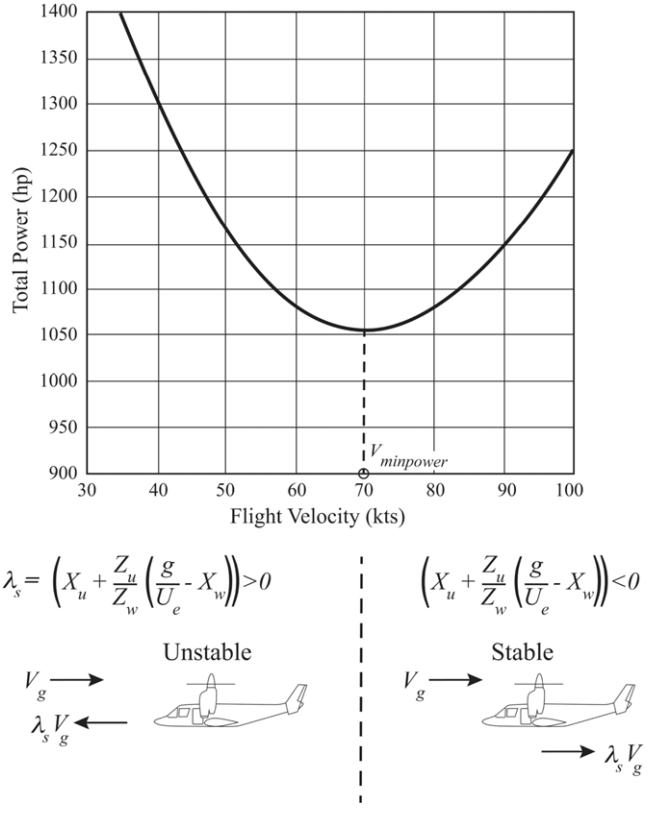

Figure 7. *Surge mode stability either side of the minimum power speed.*

leads to forward rotor disc tilt, hence k_{w0} should be negative to correct a positive w_0; $+\delta_e$ corresponds to up-elevator, hence k_{w0} should be positive to correct a positive w_0: $+X_b$ leads to $+\delta_e$ and $-B_1$, hence k_{w0} should be positive to correct a positive w_0. In all three cases, the feedback leads to a positive pitching moment to counteract the increasing (downward) w_0 perturbation. The signs of the control derivatives listed in Appendix B are summarised in Tables 1 and 2. It is particularly important to note that, from Equation (3), positive perturbations in w_0 can be caused by perturbations in incidence, $(+w/U_e)$ or pitch

Table 1. *Control derivative effects in H-mode*

	B_1	δ_e	X_b
X	−ve	+ve	+ve
Z	+ve	+ve	−ve
M	−ve	+ve	+ve

Table 2. *Feedback gains at neutral surge mode stability; FXV-15 at 55kts*

	B_1	δ_e	X_b
k_{w0}	−0.022rad/m/s	0.086rad/m/s	0.407in/m/s
	−0.6deg/100ft/min	2.5deg/100ft/min	0.2in/100ft/min

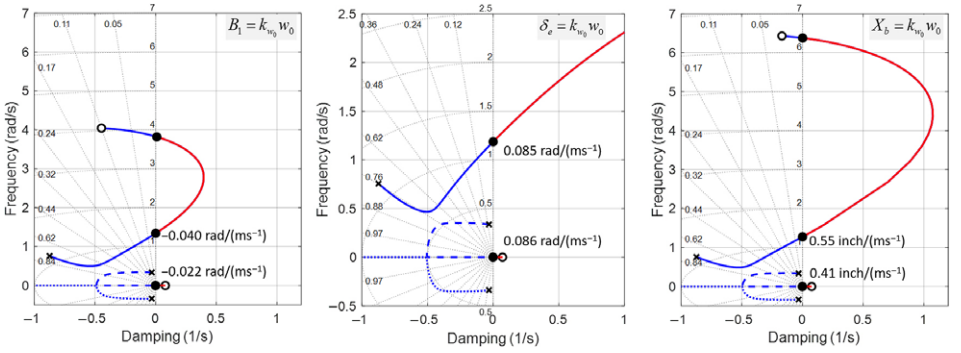

Figure 8. *FXV-15 at 55kts in H-mode; eigenvalue loci for varying gain k_{w0} with feedback to cyclic B_1, elevator δ_e and pilot's stick X_b.*

attitude, $(-U_e\theta)$. The consequences of this combined dynamic will be discussed as part of the following analysis.

With vertical velocity control given by Equation (7), the closed-loop PVS can be described by the partitioned linear differential equation,

$$\begin{bmatrix} \dot{u} \\ \dot{w} \\ \dot{q} \\ \dot{w}_0 \end{bmatrix} - \left[\begin{array}{c|ccc} X_u & X_w - \frac{g}{U_e} & X_q - W_e & \frac{g}{U_e} \\ \hline Z_u & Z_w & U_e & k_{w0}Z_{X_b} \\ M_u & M_w & M_q & k_{w0}M_{X_b} \\ Z_u & Z_w & 0 & k_{w0}Z_{X_b} \end{array}\right] \begin{bmatrix} u \\ w \\ q \\ w_0 \end{bmatrix} = \begin{bmatrix} 0 \\ 0 \\ 0 \\ 0 \end{bmatrix} \tag{8}$$

where Equation (3) has been used to substitute w_0 for θ and small terms have been neglected, e.g. sin Θ_e/U_e. The X-force control derivatives have also been neglected in the analysis as they have a minor influence on the approximations in H-mode. The eigenvalue loci for varying gains for all three feedback loops are shown for the 55kts (back side) flight case in Fig. 8. Initially, we focus discussion on the low-frequency mode. This unstable surge mode develops from the phugoid, with its stable counterpart heading to infinity on the real axis as gain increases; this is the strongly controlled flight-path mode. The unstable surge mode is located at approximately the same position in all three cases and close to the approximate value shown in Fig. 6, with $\lambda_s \approx +0.05$ ($t_D \approx 14$sec). The gains required to de-stabilise the surge mode are highlighted in Fig. 8 and summarised in Table 2. These are shown in the units used in the FLIGHTLAB analysis, and in control units per 100ft/min, a measure available to the pilot on the

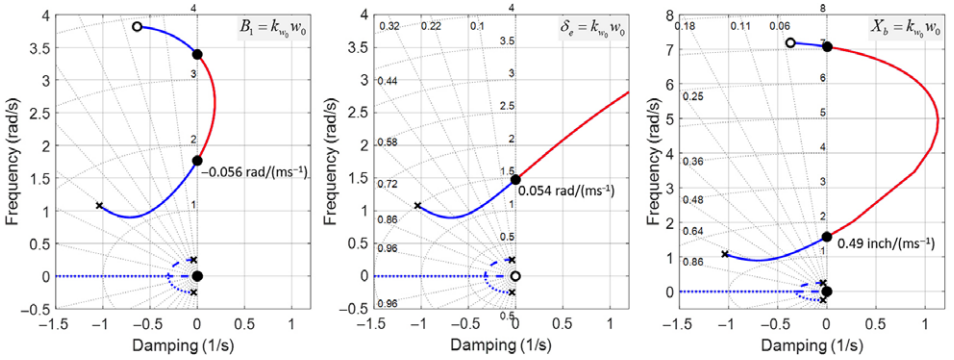

Figure 9. *FXV-15 at 75kts in H-mode; eigenvalue loci for varying gain k_{w0} with feedback to cyclic B_1, elevator δ_e and pilot's stick X_b.*

rate of climb/descent indicator. The B_1 and X_b gains can be described as low; the pilot or autopilot would not need to work hard to drive the surge mode unstable.

The behaviour of the short-period mode, the second branch of the loci in Fig. 8, warrants further discussion. But first, Fig. 9 shows the eigenvalue loci for the feedback loops at the 75kts case, on the front side of the power curve. The pattern of change for the phugoid mode is similar to the 55kts case, but the surge mode comes to rest close to neutral stability. As forward speed increases, the trim point moves further up the front side of the power curve, and the zero moves further left as the surge mode stabilises.

The theory described in Appendix A provides the framework for deriving an approximation to the surge mode stability in the case of finite gain. The conditions for the use of the approximation, based on the partitioning shown in Equation (8), are generally satisfied, even at the relatively low gain levels required to create the surge mode. The mode is separated from the short-period and flight-path modes on the plane and is dominated by u-deviations. At low-moderate gain levels, it is difficult to find an approximation for all three modes based on three-level partitioning but the two-level partitioning shown in Equation (8) gives an approximate eigenvalue in the form,

$$\lambda_s = X_u + \frac{Z_u}{Z_w}\left[-X_w + \frac{g}{U_e}\left(\frac{1}{M_{X_b} k_{w0}}\left(M_w - \frac{M_u Z_w}{Z_u}\right)\right)\right] \tag{9}$$

where X_b is used as the control variable. The limiting case given by Equation (5) emerges as $k_{w0} \to \infty$. The approximation works reasonably well for low gain values with the effective static stability moment within Equation (9) (M_{weff}) contributing to bringing the surge mode towards neutral stability, a consequence of the close coupling between surge and heave velocity. Figure 10 shows a comparison between the Equation (9) approximation and the exact surge mode eigenvalue predicted by the 3dof pitch-surge-heave dynamics for both 55kts and 75kts conditions, with w_0 feedback to X_b. The stability boundary for the 55kts case matches the result shown in Fig. 8, while the surge mode remains stable at 75kts.

Although the surge mode is a relatively benign dynamic, its insidious nature makes it very dangerous as the details in the accident reports cited in this paper demonstrate. As shown in Figs. 8 and 9, the pitch-heave short-period mode is also driven unstable and, with a period of about 10sec at 55kts, reducing with increasing flight speed, presents a different challenge to a pilot. Some insight into the reason for this loss of stability can be gained by noting that the w_0 feedback has two components; one from aircraft incidence (w/U_e), the other from pitch attitude (θ). Feedback from θ is always stabilising but it is the feedback from incidence that destabilises the short-period mode. As incidence increases, all three control feedback loops result in a pitch-up response, increasing the incidence further in the short term. The impact on the short-period mode for control with elevator differs from control with cyclic or stick. A positive (up) δ_e decreases the lift on the aircraft, as does a positive (forward) B_1. However, for flight-path control, it is the moment that defines the feedback strategy; so, positive δ_e and negative B_1 are

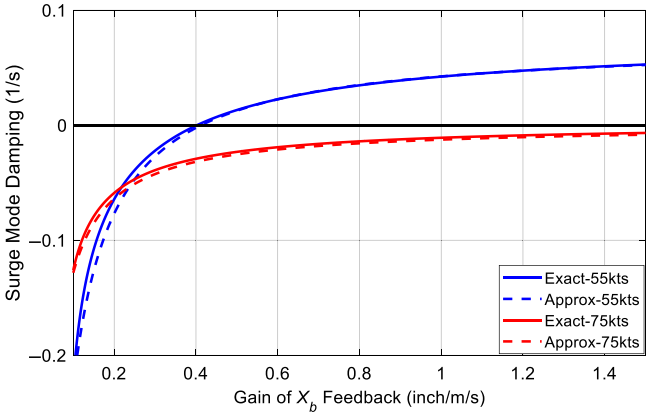

Figure 10. *Variation of approximate and 'exact' surge mode damping for the FXV-15 at 55kts and 75kts.*

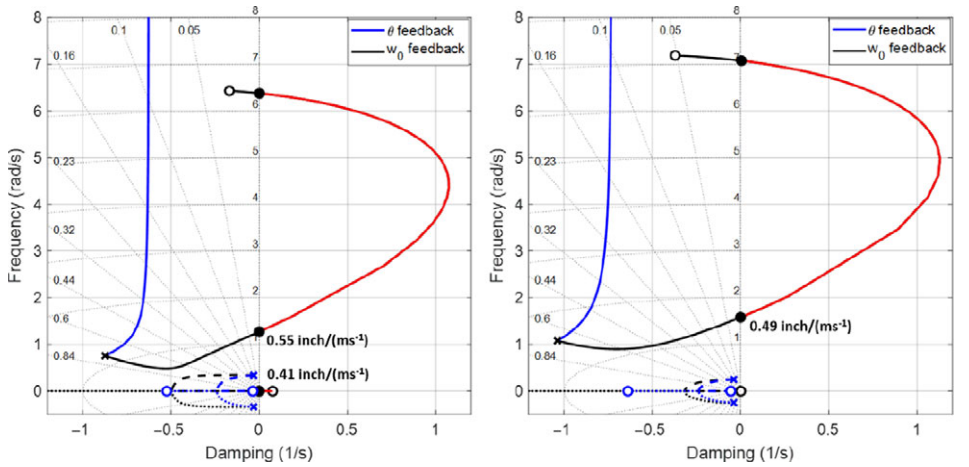

Figure 11. *Eigenvalue loci showing comparison between θ and w_0 feedback; FXV-15 in H-mode at 55kts (left) and 75kts (right).*

used. Since in H-mode at low-medium speeds, the cyclic moment is much stronger than that due to the elevator, the former dominates with X_b control. The consequence is that, as the feedback gain is increased with elevator control, the magnitude of the effective heave damping ($Z_w + k_{w0}Z_{\delta e}$) reduces. The loci for elevator control never return to the stable half of the plan as shown in Figs. 8 and 9.

Control of pitch attitude alone does not result in flight path constraint of course, but it is a much safer control strategy for a pilot to adopt for speed control, on either side of the power curve, with vertical flight path controlled with collective. Figure 11 shows a comparison of eigenvalue loci for vertical flight path (w_0) and pitch attitude (θ) feedback to stick (X_b). With θ feedback, as the gain is increased, the short-period mode frequency increases with constant damping, although reducing relative damping, hence degrading the handling qualities. Simultaneous increase of frequency and relative damping requires the addition of pitch rate feedback, or increased anticipation by the pilot.

Under the influence of the strong flight-path control, the short-period mode has changed in character and the two-level partitioning in Equation (8) cannot be further divided to isolate the unstable oscillatory mode. The conditions for weak coupling between sub-system dynamics do not apply; for example, both have a similar modulus, approximately unity in Fig. 11 at the gain for neutral stability, so they are not

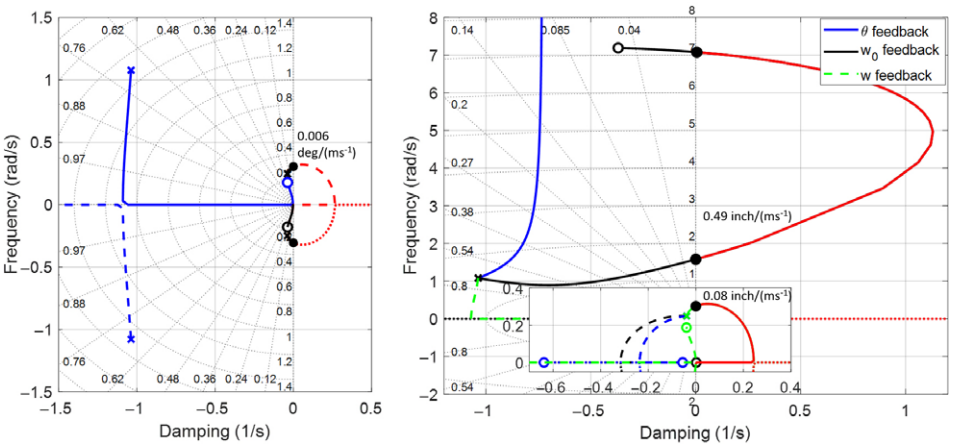

Figure 12. *Comparison of eigenvalue loci with different feedback loops; θ, w_0 and w to X_b (right) and the expanded phugoid for w to X_b (left); FXV-15 in H-mode at 75kts, 3.5deg descent.*

sufficiently separated on the eigenvalue plane. The third-order system created by the partitioning in Equation (8) has approximate eigenvalues given in the form

$$\lambda^3 + A\lambda^2 + B\lambda + C = 0 \tag{10}$$

where

$$A = -M_q - Z_w - k_{w0}Z_\eta \tag{11}$$

$$B = Z_w M_q - U_e M_w + k_{w0}Z_\eta M_q \tag{12}$$

$$C = k_{w0}U_e\left(Z_\eta M_w - M_\eta Z_w\right) \tag{13}$$

where η is used as a general control variable. According to the Routh-Hurwitz stability criteria [15], the oscillatory mode changes stability when

$$AB = C \tag{14}$$

Substituting the derivatives from Appendix B into these expressions results in close agreement with the cross-over frequencies for B_1 and X_b control shown in Fig. 11. Reasonable agreement can also be derived if we assume that the k_{w0} terms in Equations (11) and (12) are small compared with the short-period mode damping and frequency, so that the gain for neutral stability of the lower branches in Fig. 11 is then approximated by the expression

$$k_{w0} \approx \left[-\left(M_q + Z_w\right)\left(Z_w M_q - U_e M_w\right) / \left(U_e\left(Z_\eta M_w - M_\eta Z_w\right)\right)\right] \tag{15}$$

For the 55kts flight speed, this corresponds to $k_{w0} = 0.5$in/m/sec, only 10% lower than the exact result in Fig. 11. Flight-path control by cyclic or elevator is natural for both fixed-wing and rotary-wing aircraft at higher flight speeds, e.g. terrain-following, and such low-frequency guidance strategies should not present a problem for pilots. However, when manoeuvring in turbulence to maintain a constant vertical rate, e.g. optimum climb or descent profiles, the strategy not only risks surge mode instability but a divergent oscillatory mode. The absence of any discussion on this problem in most of the standard flight dynamics textbooks is surprising. Reference [16] does discuss the surge mode instability resulting from controlling the vertical flight-path and even shows the short-period mode being driven unstable in the relevant system survey diagram common in that text, but without comment. Figure 12 shows a comparison of the eigenvalue loci for the components of w_0 feedback to X_b with the w feedback case expanded. This shows the stick being pulled back to counteract the increase in w

(incidence). The phugoid mode is now driven unstable, demonstrating the failure of this feedback loop in isolation.

The modal pattern under closed-loop control for the tiltrotor in H-mode closely resembles the results for a conventional helicopter presented in [5] and [12]. In C-mode, new dynamics come into play which will now be explored.

2.3 Constrained flight-path control in C-mode

The eigenvalue loci as a function of speed, for the FXV-15 in C-mode, with nacelle angle at 60deg (i.e. tilted forward 30deg) are shown in Fig. 13. The aircraft is trimmed in a 3.5deg descent angle and the flap setting is 40deg. The speed range shown corresponds to flight just below and extended above the minimum power speed shown in Fig. 3.

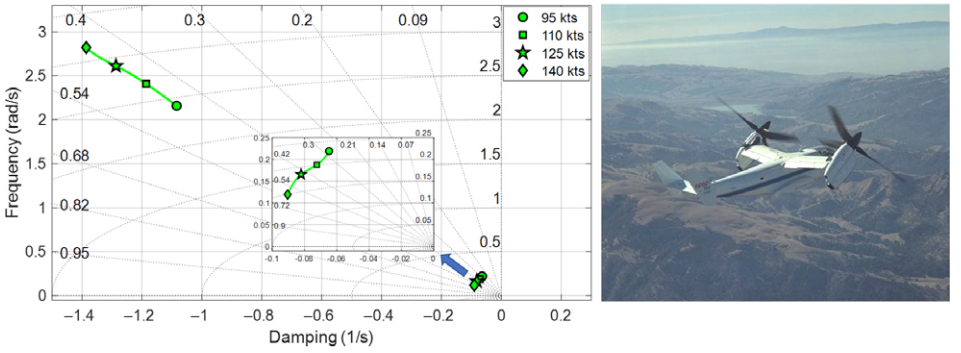

Figure 13. *Longitudinal eigenvalues as a function of speed for the FXV-15 in C-mode, 60deg nacelle angle, flap setting 40deg, flight-path angle 3.5deg descent. XV-15 in C-mode (photo NASA).*

Based on the minimum power shown in Fig. 3, the 95kts and 105kts conditions are selected for feedback analysis. As discussed earlier, in C-mode both cyclic pitch and elevator are connected to the pilot's control stick, with the gearing to cyclic reducing as a function of nacelle angle. The eigenvalue loci for varying feedback gains at the 95kts flight condition are shown in Fig. 14. The striking difference with the H-mode case below minimum power is the absence of the unstable surge mode. The reason for this can be found within the approximation for the surge mode in Equation (9). The derivative X_w changes character markedly as the nacelles tilt forward. A perturbation in w now leads to an increase in rotor thrust, as in H-mode due to the inflow dynamic; but the thrust now has a large component in the fuselage x-direction. The derivative tables in Appendix B show that X_w changes from -0.012/sec in H-mode at 75kts to $+0.143$/sec in C-mode at 95kts; a sign change and order-of-magnitude increase. The surge mode still exists as the gain increases, but remains stable. Cyclic pitch control no longer destabilises the short-period mode as the pitching moments from the proprotors strengthen the natural static stability (M_w) to overpower the incidence destabilising feedback. Elevator control remains destabilising for the short-period mode, however, with destabilising gain of 3.5deg/100ft/min, or 2.5deg/deg of flight-path angle change. The pilot's control is therefore destabilising with cross-over gain of about 1in/deg of flight-path angle.

The patterns described for the 95kts case are repeated at 105kts with similar conclusions. At both speeds, pitch attitude feedback to elevator or stick is stabilising, as in H-mode. For completeness, comparisons of θ and w_0 feedback loci are shown in Fig. 15, with a similar pattern to the H-mode results in Fig. 11. The w_0 feedback gains for short-period neutral stability can be derived using the approximate Routh-Hurwitz formulae in Equation (15).

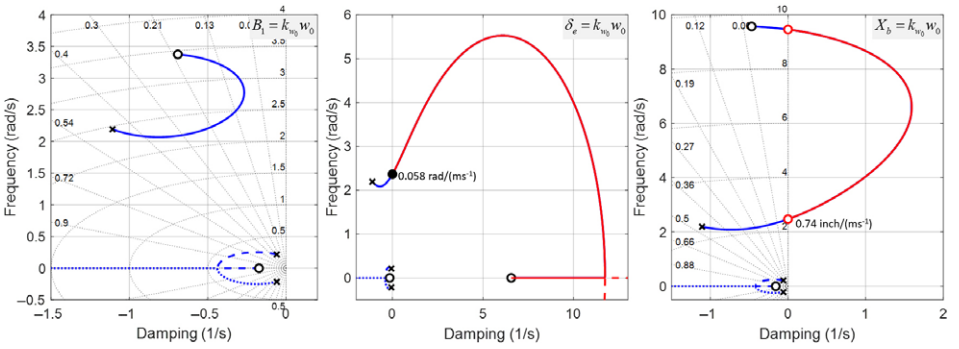

Figure 14. *FXV-15 at 95kts in C-mode, nacelle angle 60deg, flap 40deg, descent angle 3.5deg; eigenvalue loci for varying gain k_{w0} with feedback to cyclic B_1, elevator δ_e and pilot's stick X_b.*

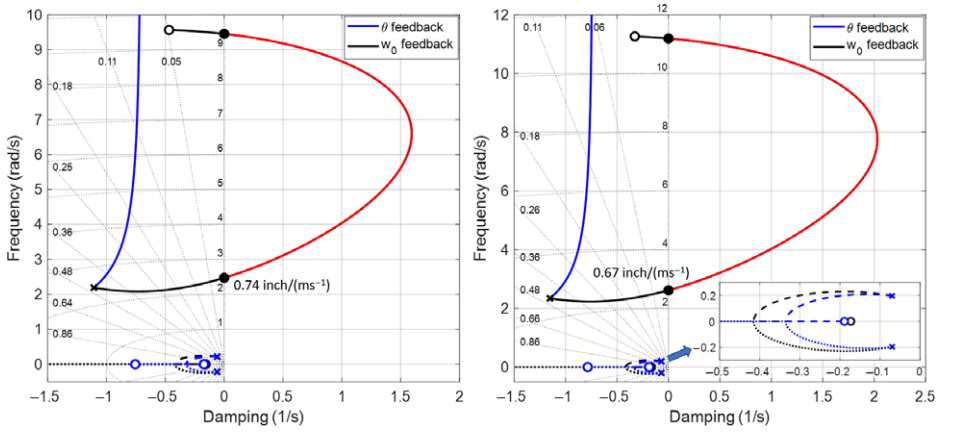

Figure 15. *Eigenvalue loci showing comparison between pitch attitude and vertical velocity feedback; FXV-15 in C-mode with 60deg nacelle, 3.5deg descent at 95kts and 105kts.*

2.4 Constrained flight path control in A-mode

Examination of closed-loop control of flight path with elevator for the FXV-15 in A-mode reveals new characteristics that further mitigate the adverse effects on surge mode stability. The longitudinal eigenvalues are shown as a function of flight speed in Fig. 16.

Based on the power curves in Fig. 3, the 135kts and 180kts airspeeds are selected as points below and above the minimum power condition. Figure 17 illustrates the eigenvalue loci for w_0 feedback to pilot's stick for these two cases, with the aircraft on a 3.5deg descent trajectory. Under strong control, the surge mode is stable at both airspeeds, with a time to half-amplitude of about 2sec at the 135kts condition. The reason the surge mode remains stable below minimum power is mainly due to the large value of the drag derivative X_u. The surge mode approximation in Equation (9) works reasonably well in A-mode as shown in Fig 18. At 135kts, the error is about 20% but the trend follows the exact results as gain is increased. In [5], the first author discussed the contribution to the drag derivative, X_u, from the propeller of a turboprop-powered aircraft. With constant power propulsion, the thrust decreases following a u perturbation, hence increasing the magnitude of X_u. However, the XV-15 features a rotorspeed governor that acts through collective pitch feedback; a positive u perturbation initially reduces both thrust and rotorspeed, leading to a further reduction in thrust as the proprotor collective pitch is reduced to maintain rotorspeed. The sensitivity of rotor thrust to collective is similar in A-mode and H-mode, impacting

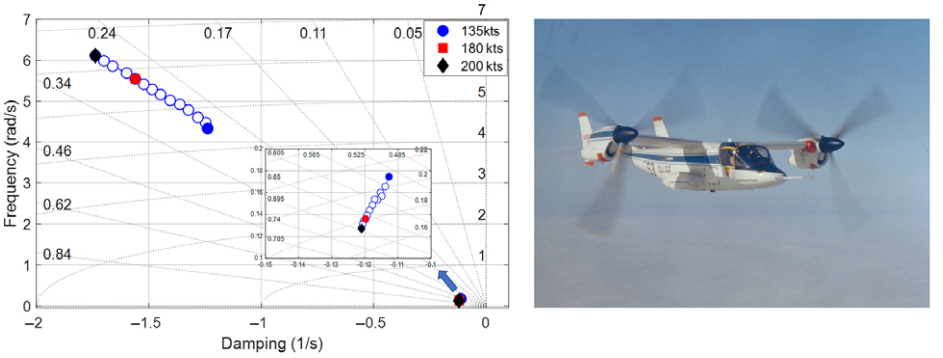

Figure 16. *Longitudinal eigenvalues as a function of speed for the FXV-15 in A-mode, flap setting 40deg, flight-path angle 3.5deg descent. XV-15 in A-mode (photo NASA).*

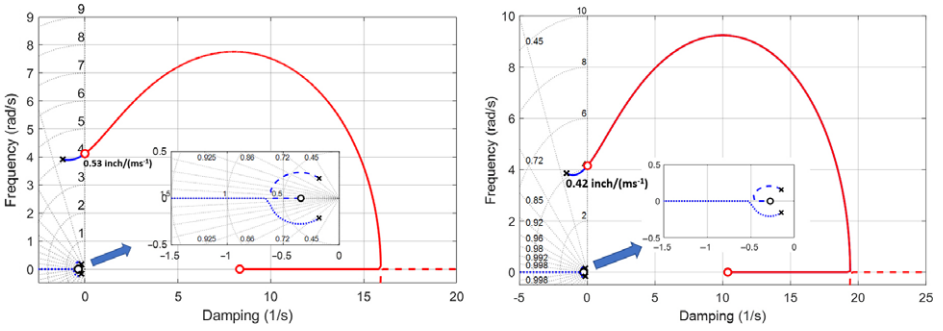

Figure 17. *Eigenvalue loci for FXV-15 longitudinal modes with w_0 feedback to stick (X_b) in A-mode, 135kts (left), 180kts (right), 3.5deg descent angle.*

different control derivatives of course ($X_{\theta 0}$ *cf.* $Z_{\theta 0}$), therefore strongly augmenting the drag derivative in A-mode.

The short-period mode is driven unstable at relatively low values of gain at both flight conditions (0.53in/m/s, 0.42in/m/s). Just as in H-mode and C-mode, controlling flight path with elevator will risk PIO tendency and eventually instability with these levels of gain.

It is emphasised that the analysis and results for the impact of closed-loop control of flight path on aircraft stability relate to the FXV-15 Level-2 complexity model [5], developed within the FLIGHTLAB [17] simulation environment. In H-mode, the surge instability for flight below minimum power closely matches the results for conventional helicopters. In C- and A-modes, mitigating aerodynamic effects reflected in the variation of stability derivatives, X_w and X_u, mean that the surge mode remains stable under strong flight-path control. This does not mean that flight-path control with centre stick below minimum power, for example on the approach or climb-out, or cruising for maximum endurance, does not have safety consequences. In all cases, the low-frequency dynamics contain a surge mode with relatively low damping, and the flight-path response to stick is opposite on the two sides of the minimum power speed. Energy management with combined cyclic/elevator and collective/thrust is the only safe strategy to adopt in this flight regime. Short-term corrective control of pitch attitude with cyclic/elevator has been shown to be a successful stabilisation strategy, but this does not replace the need for coupled-control for the management of flight path and airspeed.

The destabilising influence of strong flight-path control with elevator on the pitch-heave short-period mode has been demonstrated for flight on both back and front sides of the power curve in all three

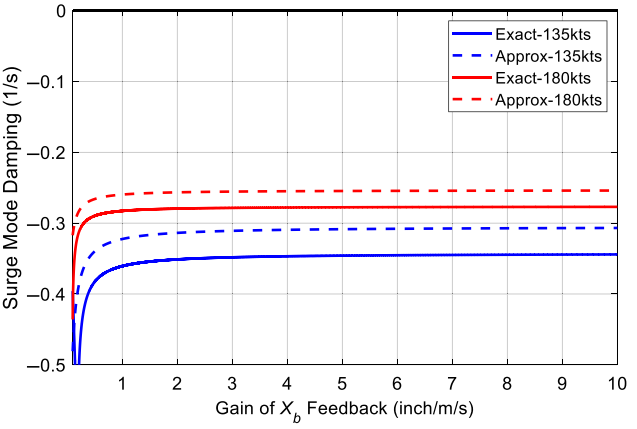

Figure 18. *Surge mode stability under flight path control; FXV-15 in A-mode.*

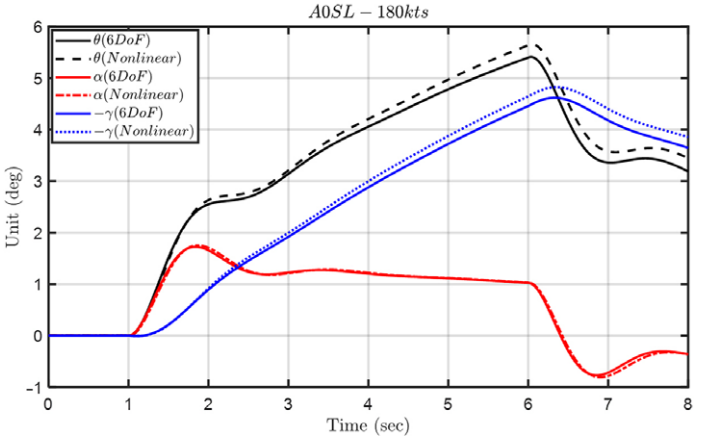

Figure 19. *Responses to 0.25inch X_b step input; comparison of linear (6dof) and nonlinear FXV-15 in A-mode at 180kts for θ, and γ.*

tiltrotor modes. The source of the problem is the feedback from the incidence component of flight path; the corrective moment for flight-path deviations resulting in an increased excursion of incidence. An equivalent interpretation is expressed in terms of the lag in the flight-path response, relative to pitch attitude, as shown in Fig 19. Flight-path angle γ lags the pitch attitude θ by about 1sec, so feedback from γ is equivalent to feeding a lagged θ, the opposite of anticipation. Figure 19 also shows the good comparison between the nonlinear FXV-15 and the 6dof linear model, reinforcing the utility of the latter for small-amplitude response analysis, in addition to stability. The θ response shows the classic drop-back characteristic as the control pulse is removed at 6sec, which also requires pilot anticipation when commanding a change in attitude or flight-path angle. References [18] and [19] examine this dynamic, describing handling qualities criteria for short-term pitch control and including a proposal for a metric based on the time to achieve a flight-path angle change. The adoption of any handling qualities metric related to flight-path control should clearly be evaluated for the connection with the APCs described in this paper.

The analysis above shows that the level of pilot/autopilot gain required to destabilise the short-period mode is similar to that for the surge mode destabilising. A successful control strategy based on flight

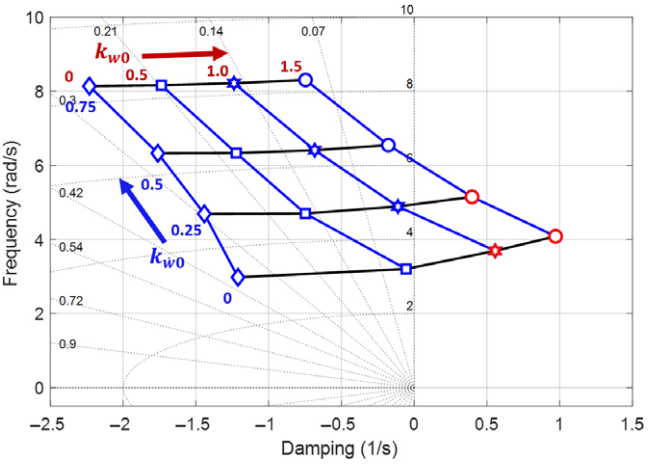

Figure 20. *Short-period pitch-heave mode eigenvalue loci map for varying feedback of vertical velocity and acceleration to X_b; FXV-15 in A-model, 135kts, $\gamma = 3.5$deg.*

path would need to include pilot anticipation, or feedback of flight-path rate (normal acceleration), as in Equation (16), and as illustrated in Fig. 20 for the 135kts A-mode flight case. A relatively small amount of anticipation (0.5in/m/s^2) would be required to recover the natural short-period damping from the neutral stability case with proportional control ($k_{w0} = 0.5$inch/m/s).

$$X_b = k_{w0} w_0 + k_{\dot{w}0} \dot{w}_0 \tag{16}$$

The guidance for requirements on flight-path stability and response to elevator for US military fixed-wing aircraft is described in MIL-HDBK 1797 [20]. Here, the issues relating to flight on the front side and back side of the power curve are discussed, particularly with application to flight-path control on the approach, for example to an aircraft carrier. The key metric defining handling quality is the flight path change to elevator/speed change at constant power. In [20], a positive flight-path angle denotes a climb, so opposite to the sense used in this paper. On the back side, the flight-path angle decreases (descent) with speed reduction, and increases (climb) with speed increase, at constant power. The reverse occurs on the front side. To quote from [20],

"*Flight-path stability is defined in terms of flight-path-angle change with airspeed when regulated by use of the pitch controller only (throttle setting not changed by the crew). For the landing approach Flight Phase, the curve of flight-path angle versus true airspeed shall have a local slope at V_{0min}.* (minimum approach speed) *that is negative or less positive than. . .*" the values given in Table 3 below in terms of HQ levels. The values relate to the slope of the flight-path vs speed curve below minimum power and are essential conditions on trim, rather than stability. Ref [20] makes the link with stability of closed-loop control by drawing on Neumark's analysis [8] to approximate the slope metric in terms of stability derivatives as given in Equation (17). The metric is proportional to the surge mode approximation and corresponding HQ boundary values are included in Table 3.

$$\frac{d\gamma}{du} = \frac{1}{g}\left[X_u - \left(X_w - \frac{g}{U_e}\right)\frac{Z_u}{Z_w}\right] \tag{17}$$

In contrast, the US military helicopter handling qualities standard (ADS-33, [21]) addresses flight-path control on the back side in terms of response to collective. The flight-path/vertical-rate response to collective *'should have a first-order appearance for at least 5sec following a step input.'* Ref [21] also states that *'pitch attitude excursions shall be limited so that they have a negligible effect on the vertical rate response.'* So, the cyclic is expected to be active in this test for the purposes of minimising

Table 3. *Flight-path angle change for different HQ levels [20] and associated surge eigenvalues*

Level 1	0.06deg/kt	$\lambda_s \approx 0.005$/sec
Level 2	0.15deg/kt	$\lambda_s \approx 0.013$/sec
Level 3	0.24deg/kt	$\lambda_s \approx 0.02$/sec

pitch attitude changes. For front-side operations, the HQ metric is quantified in terms of the flight-path response lag. To quote again from [21]; *'The vertical rate response shall not lag the pitch attitude response, with the collective controller held fixed, by more than 45 degrees at all frequencies below 0.40 rad/sec for Level 1 and 0.25 rad/sec for Level 2.'* Of course, these criteria reflect the open-loop response of the aircraft and do not address the question of how such criteria might impact closed-loop operations, to minimise or eliminate the potential for flight-path related APCs.

The control of flight-path angle with elevator or cyclic has also revealed a loss of stability of the short-period mode across all three tiltrotor configurations, on the back and front side of the power curve, caused by the implicit feedback of the incidence component within γ. It has been shown that the instability can be avoided by the pilot or autopilot applying anticipation (normal acceleration feedback) but the underlying problem remains. As noted above, the first author explored the development of HQ metrics for pitch and flight-path control of tiltrotors in [19], proposing a metric combining control-anticipation with flight-path delay. However, this research did not specifically address the connection with APCs and the loss of stability described in this paper. It is recommended that this topic is explored more extensively to determine the safe limits on closed-loop control of vertical flight path for tiltrotor aircraft.

3. Constrained roll control and yaw divergence

3.1 A well-understood problem for some fixed-wing aircraft

The flight control and handling problems associated with adverse-yaw due to aileron deflection have been infamous in aeronautical history. The Wright brothers first experienced the effect on their 1901 glider [22]; Wilbur noted in a presentation that '*We proved that our machine does not turn towards the* lowest *wing under all circumstances, a very unlooked for result and one which completely upsets our theories as to the causes which produce the turning to right or left.'* They designed their 1902 glider and powered Flyer family with an interlink between wing-warp and rudder [23] and [24]; there was no separate yaw control on these aircraft. The re-occurrence of the problem on different types over the first 70 years of aviation led to adverse-yaw being recognised as a practical handling problem needing attention in the design of military fixed-wing aircraft [20]. A theory was developed by Pinsker [7] to predict what he described as a 'minimum acceptable value' for weathercock stability, N_v, in the presence of adverse-yaw from aileron deflection, ξ. Pinsker's theory predicted that under strong control of roll, the yaw would diverge when the effective weathercock stability reduced to zero; the condition for stability becoming,

$$\overline{N}_v = \left(N_v - \frac{N_\xi}{L_\xi} L_v \right) > 0 \tag{18}$$

As with Neumark's approximation [8] for surge-mode stability, Equation (5), the complex combination of pilot and aircraft control is reduced to the behaviour of a single effective derivative in Equation (18). MIL-STD 1797 [20] frames the 'problem' in terms of the lateral control divergence parameter (LCDP), essentially the same as Pinsker's effective stability derivative, and describes examples of aircraft that featured rudder shaping to reduce adverse-yaw and improve so-called nose-slice departure resistance.

3.2 Application to tiltrotor aircraft

The first author reported analysis of the impact of adverse-yaw on tiltrotor stability in airplane mode using the FXV-15 in [5]. The analysis is extended here, in the notation of [5], with aileron deflection denoted by η_a, rudder deflection by η_r, differential (proprotor) collective pitch (DCP) by θ_{0D}. First, the constrained flight analysis to derive Pinsker's effective directional stability is described. The linear equations for small perturbation, lateral-directional motion (sway v, roll rate and angle p and ϕ, yaw rate r), with associated stability and control derivatives, can be written as

$$\begin{bmatrix} \dot{v} \\ \dot{p} \\ \dot{\phi} \\ \dot{r} \end{bmatrix} - \begin{bmatrix} Y_v & Y_p + W_e & g\cos\Theta_e & Y_r - U_e \\ L_v & L_p & 0 & L_r \\ 0 & 1 & 0 & 0 \\ N_v & N_p & 0 & N_r \end{bmatrix} \begin{bmatrix} v \\ p \\ \phi \\ r \end{bmatrix} = \begin{bmatrix} Y_{\eta_a} & Y_{\eta_r} \\ L_{\eta_a} & L_{\eta_r} \\ 0 & 0 \\ N_{\eta_a} & N_{\eta_r} \end{bmatrix} \begin{bmatrix} \eta_a \\ \eta_r \end{bmatrix} \tag{19}$$

or, more generally, with stability and control matrices $\boldsymbol{A}$ and $\boldsymbol{B}$

$$\frac{d\mathbf{x}}{dt} - \mathbf{A}\mathbf{x} = \mathbf{B}\mathbf{u} \tag{20}$$

Pinsker assumed that, in the limit of infinitely strong control, a pilot could effectively suppress the roll motion with ailerons, so that the roll equation could be written as a quasi-steady relationship between the sway and yaw motions and the aileron deflection

$$L_v v + L_r r + L_{\eta_a}\eta_a = 0 \tag{21}$$

With constrained roll motion, and neglecting the small $Y_p + W_e$ term, the sway and yaw equations take the form

$$\begin{aligned} \dot{v} - Y_v v + U_e r &= 0 \\ \dot{r} - \overline{N}_v v - \overline{N}_r r &= 0 \end{aligned} \tag{22}$$

where the compound yaw derivatives are the effective directional stability and yaw damping, augmented by the aileron control, and given by the expressions

$$\overline{N}_v = N_v - \frac{N_{\eta_a}}{L_{\eta_a}} L_v;\ \overline{N}_r = N_r - \frac{N_{\eta_a}}{L_{\eta_a}} L_r \tag{23}$$

Combining Equations (21) and (22), yaw motion is then described by the second-order equation

$$\ddot{r} - \left(\overline{N}_r + Y_v\right)\dot{r} + \left(\overline{N}_v U_e + Y_v \overline{N}_r\right) r = 0 \tag{24}$$

In many fixed-wing aircraft, the product $Y_v\overline{N}_r$ is small compared with the $\overline{N}_v U_e$ term, so the effective directional stiffness is approximated by $\overline{N}_v U_e$. The condition for directional stability is then given by Pinsker's expression

$$\overline{N}_v = \left(N_v - \frac{N_{\eta_a}}{L_{\eta_a}} L_v\right) > 0 \tag{25}$$

This effective directional stability depends on the sign of N_{η_a}; negative (adverse aileron-yaw) and stability is reduced; positive (proverse aileron-yaw) and the coupling increases the yaw stability. Normally for fixed-wing aircraft, N_{η_a} is negative and, at high angles of attack, natural directional stability N_v can also reduce (fin-shielding effect) and the ratio of control derivatives in Equation (25) can become so large that the coupling term overpowers the natural stability. Strong control by the pilot attempting to maintain roll attitude can then lead, in the limit, to the 'nose-slice' yaw departure.

How this might translate into tiltrotor flight dynamics can be explored using the FXV-15. The flight condition examined is a 280kts straight and level flight condition at sea-level. The $\boldsymbol{A}$ and $\boldsymbol{B}$ matrices

corresponding to this flight condition are

$$\boldsymbol{A} = \begin{bmatrix} -0.36 & -6.4 & 9.8 & -137 \\ -0.071 & -1.34 & 0 & -0.19 \\ 0 & 1 & 0 & 0 \\ 0.072 & -0.184 & 0 & -1.21 \end{bmatrix} \tag{26}$$

and

$$\boldsymbol{B} = \begin{bmatrix} -0.52 & -12.07 & -6.68 \\ 5.17 & -1.17 & 22.04 \\ 0 & 0 & 0 \\ -0.183 & 6.78 & 40.7 \end{bmatrix} \tag{27}$$

where the control vector contains three controls; the aileron, rudder and differential collective pitch (DCP or θ_{0D}).

$$\boldsymbol{u} = \begin{bmatrix} \eta_a \\ \eta_r \\ \theta_{0D} \end{bmatrix} \tag{28}$$

For the XV-15 in A-mode, roll control is achieved through aileron only and yaw control is achieved through rudder only. In contrast, with Leonardo's AW609 tiltrotor, DCP provides the yaw control function. In the present study, the FXV-15 H-mode DCP range (±1.6deg) is retained in A-mode but inputs are only made through an interlink with aileron (±19deg) to provide the mechanism for coupled roll yaw, hence adverse or proverse aileron-yaw. To examine the impact of this coupling, the rudder function is not activated in the feedback loop, or by the pilot. From the $\boldsymbol{B}$ matrix, the FXV-15 has a small natural adverse aileron-yaw (element 4,1), but the ratio N_{η_a}/L_{η_a} is only 0.04, so the effective directional stability (Equation (25)) is only 5% less than the natural directional stability, N_v. There should be no risk of adverse roll-yaw coupling reducing the directional stability with strong roll control for the XV-15 in this flight condition.

The control law to be investigated is one where the pilot (or automatic FCS) controls roll attitude with aileron, coupled with the feed forward to DCP, θ_{0D}, through the combined proportional forms

$$\begin{aligned} \eta_a &= k_\phi \phi \\ \theta_{0D} &= k_1 \eta_a \end{aligned} \tag{29}$$

To achieve stabilisation with ϕ control, the feedback to aileron is negative; i.e. $k_\phi < 0$. The interlink coupling that applies adverse-yaw is achieved with $k_1 < 0$. For the case with no interlink, $k_1 = 0$, the eigenvalue loci are shown in Fig. 21, with points shown for k_ϕ values up to −1.0deg/deg. The attitude feedback leads to the spiral and roll subsidence modes combining into a yaw-sideslip oscillation with frequency and damping, in the limit of infinite gain, given by Equation (24). This closed-loop zero is essentially the Dutch roll mode free of roll motion, highlighting that the frequency of the Dutch roll is well predicted by the approximation. Reference [20] (MIL-HDBK 1797) makes the point that the propensity to nose slicing is related to the separation of the open-loop Dutch roll mode and this closed-loop zero. In the limit, the Dutch roll mode itself transforms into a roll oscillation with damping given by $-L_p/2$ and infinite frequency. As expected, there is no instability resulting from the adverse-yaw of the FXV-15 for the case $k_1 = 0$.

With aileron-DCP coupling increased to $k_1 = -0.08$deg/deg, the eigenvalue loci transform as shown in Fig. 22. For every +1.0deg of aileron, the interlink now applies −0.08deg of DCP, resulting in negative yawing and rolling moments. $L_{\theta 0D}$ is naturally positive, from the changing in-plane lift forces on the proprotor; positive DCP results in an up-force on the left rotor and down-force on the right rotor. We now see a situation where the adverse-yaw has increased 20-fold and the effective roll control sensitivity

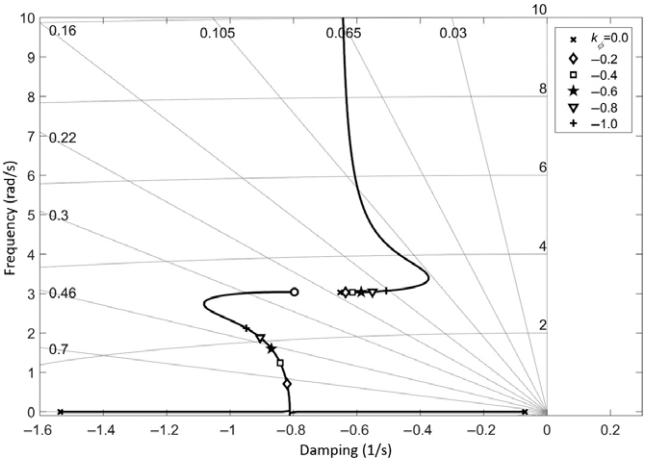

Figure 21. *Eigenvalue loci for FXV-15 lateral-directional dynamics with varying* k_ϕ; $k_1 = 0$.

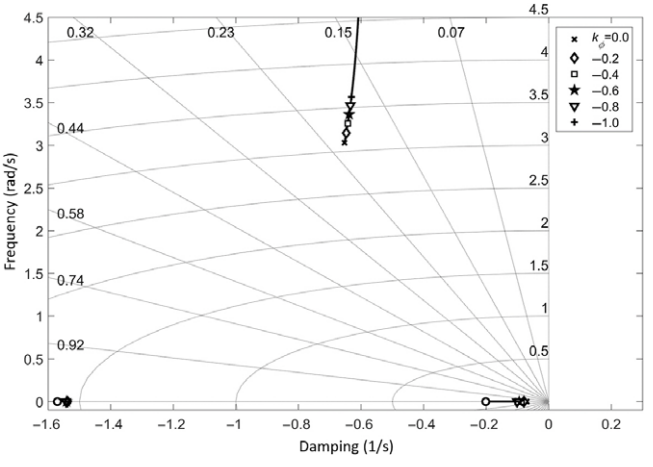

Figure 22. *Eigenvalue loci for FXV-15 lateral-directional dynamics for varying* k_ϕ; $k_1 = -0.08$.

has reduced to 66% of the value with $k_1 = 0$. The topology of the loci changes, the spiral and roll modes moving only slightly on the real axis, morphing into yaw-sway subsidence modes. The loci for the oscillatory roll mode show a similar pattern to $k_1 = 0$, both damping and relative damping decreasing with increasing gain.

From Equation (24), the approximation to the two subsidences at high gain can be written as

$$\lambda^2 + (\overline{N}_r' + Y_v)\lambda + (\overline{N}_v' U_e + Y_v \overline{N}_r') = 0 \tag{30}$$

where the effective yaw stiffness and damping are given by the expressions

$$\overline{N}_v' = N_v - \frac{\overline{N}_{\eta_a}}{\overline{L}_{\eta_a}} L_v; \quad \overline{N}_r' = N_r - \frac{\overline{N}_{\eta_a}}{\overline{L}_{\eta_a}} L_r \tag{31}$$

with the compound control derivatives

$$\begin{aligned} \bar{L}_{\eta_a} &= L_{\eta_a} + k_1 L_{\theta 0D} \\ \overline{N}_{\eta_a} &= N_{\eta_a} + k_1 N_{\theta 0D} \end{aligned} \tag{32}$$

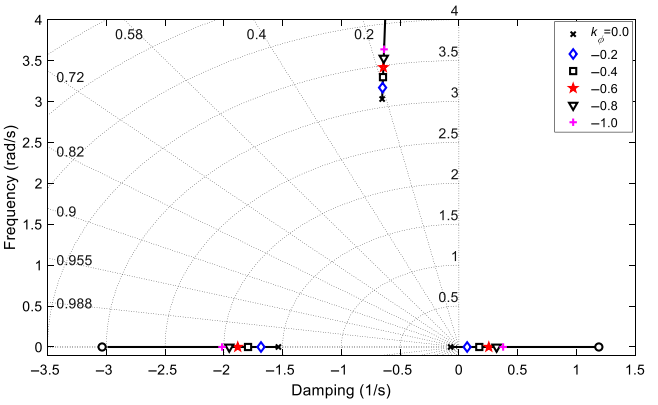

Figure 23. *Eigenvalue loci for FXV-15 lateral-directional dynamics for varying k_ϕ; $k_1 = -0.1$.*

Using the derivative values from the ***A*** and ***B*** matrices, the approximate zeros on Fig. 22 are,

$$\lambda_1 = -1.5; \quad \lambda_2 = -0.27; \tag{33}$$

The effective directional stability (Equation (25)) is close to zero, with the only stabilising effect coming from the product of the sway and (effective) yaw damping. Also, the ratio of effective yaw to roll control (from Equation (32)) is about 1. Adverse-yaw contributed by the DCP is now acting like the adverse aileron-yaw described in [7].

Increasing the coupling into DCP from aileron has a predictable impact. The results for $k_1 = -0.1$deg/deg are shown in Fig. 23. The attitude feedback control now drives the yaw-sway mode unstable, with approximations for the closed-loop zeros again given by the solutions to Equation (30),

$$\lambda_1 = -2.7; \quad \lambda_2 = +0.8; \tag{34}$$

The agreement with Fig. 23 is reasonable, although the strength of the unstable mode is under-predicted by about 30%. Nevertheless, the fundamental physical mechanism of the instability is captured by the approximation. From Equation (25), the lower the natural directional stability N_v, then the smaller the adverse-yaw, from either natural aerodynamics or control couplings, is required to drive the mode unstable.

The analytic approximation above represents the limiting case of infinitely strong control of roll attitude with aileron. As with strong vertical flight-path control discussed in the first part of the paper, the approximation for finite-gain control by the pilot or an automatic FCS, can be derived from a partitioned form of the equations of motion; separating the strongly controlled roll motion from the weakly controlled sway-yaw motion. Re-arranging the equations of motion, Equation (19), into weakly and strongly controlled states, gives the new closed-loop ***A*** matrix

$$\begin{bmatrix} \dot{v} \\ \dot{r} \\ \hline \dot{p} \\ \dot{\phi} \end{bmatrix} - \left[\begin{array}{cc:cc} Y_v & Y_r - U_e & Y_p + W_e & g\cos\Theta_e \\ N_v & N_r & N_p & \bar{N}_{\eta_a} k_\phi \\ \hdashline L_v & L_r & L_p & \bar{L}_{\eta_a} k_\phi \\ 0 & 0 & 1 & 0 \end{array}\right] \begin{bmatrix} v \\ r \\ \hline p \\ \phi \end{bmatrix} = \begin{bmatrix} 0 \\ 0 \\ \hline 0 \\ 0 \end{bmatrix} \tag{35}$$

As discussed in Appendix A, the conditions for the approximation to work are that the eigenvalues of the sub-systems and their modal content are separated and the couplings between the weakly and strongly controlled dynamics are small. As gain is increased, both conditions become increasingly valid. Neglecting some of the small terms, e.g. Y_p, the approximating quadratics for the low modulus (λ_1) and

high modulus (λ_2) eigenvalues can be written as

$$\lambda_1^2 - \left(Y_v + \overline{N}'_v - g\frac{L_v}{k_\phi \bar{L}_{\eta_a}}\right)\lambda_1 + \left(\overline{N}'_v U_e + Y_v \overline{N}'_r\right) + \frac{g}{k_\phi \bar{L}_{\eta_a}}\left(\overline{N}'_v L_r - \overline{N}'_r L_v\right) = 0 \tag{36}$$

$$\lambda_2^2 - L_p \lambda_2 - k_\phi \bar{L}_{\eta_a} = 0 \tag{37}$$

The roots of Equation (36) converge to those of Equation (30) as gain k_ϕ increases, one solution becoming positive (yaw-sway divergence) as the gain increases. The value of gain k_ϕ for neutral stability can be found by setting the stiffness term in Equation (36) to zero, i.e.

$$k_\phi = -\frac{g}{\bar{L}_{\eta_a}} \frac{\left(\overline{N}'_v L_r - \overline{N}'_r L_v\right)}{\left(U_e \overline{N}'_v + Y_v \overline{N}'_r\right)} \tag{38}$$

With further simplification, a more concise expression captures the main effect

$$k_\phi \approx g \frac{\overline{N}'_r L_v}{\bar{L}_{\eta_a} U_e \overline{N}'_v} \tag{39}$$

The yaw derivatives now include the interlinked DCP control (from Equations (31) and (32)). For the case with $k_1 = -0.1$, the gain value for neutral stability is -0.09deg/deg from Equation (38), and -0.07deg/deg from the simple approximation in Equation (39). This relatively simple expression can be used to establish the destabilising gain for different values of k_1 and the effective aileron-yaw $\overline{N}_{\eta_a}$. Noting the aileron control gearing of 3.9deg/inch of pilot stick, when seen as a pilot feedback, the gains are low. The dominant effect is, of course, the coupling into DCP which has a roll control sensitivity more than four times greater than the aileron. The simplified Equation (39) also links with the original Pinsker result; zero effective directional stability equates to infinitely strong roll control ($k_\phi \to \infty$). Rearranging the terms in Equations (31) and (32), an expression for the level of coupling required to produce neutral stability, as a function of the stability and control derivatives can be derived in the form of Equation (40), showing the importance of the ratios of static stability derivatives N_v and L_v.

$$k_1 = -\frac{N_{\eta_a} - \frac{N_v}{L_v} L_{\eta_a}}{N_{\theta_{0D}} - \frac{N_v}{L_v} L_{\theta_{0D}}} \tag{40}$$

The presence of other inputs into the roll channel has not been investigated, but are likely to modify the results and make the problem considerably more complicated. For example, the addition of stability augmentation through increased roll damping will position the eigenvalues of the modes further to the left on the complex plane; but eventually the attitude feedback will overpower the rate stabilisation in the presence of adverse aileron-yaw. The addition of other DCP inputs, for example for structural load alleviation, as discussed in [5], or to minimise torque splitting during turns, have also not been explored. These are important since their presence will influence the amount of DCP available for the primary flight control through the interlink with aileron. Any rate limiting in the actuation system will further complicate the problem. To quote from [1], *'These features combine to make PVS behavior at the margins of the control-effector/control-function envelope a multidimensional surface of bewildering complexity.'* The analysis described in this paper is essentially linear so it cannot contribute to understanding the impact of these additional features.

How might this adverse coupling be experienced by a pilot? If they are struggling to maintain roll attitude, then, with the addition of adverse-yaw, the threatening yaw-sway divergence should be apparent. In the fixed-wing carrier approach scenario, controlling horizontal flight path through roll control is paramount, so the pilot must find a compensatory technique in the presence of the incipient APC. Yaw compensation with pedals is the obvious strategy but the phasing with roll control will be important for the outcome, because this motion is superimposed on the oscillatory roll. Any pedal inputs intended to counteract the oscillatory yaw could suppress or exacerbate the divergent motion, depending on their phase with the roll motion and roll control inputs.

The results from the above study of the impact of adverse-yaw on the directional stability of the FXV-15 are certainly compelling. However, it is stressed that the validation of the FXV-15 with flight-test data, reported in [5], is very limited. Furthermore, the analysis carried out has been linear, so it is strictly only applicable to small-amplitude stability and response. The results are indicative, but the problems they express are often inherently nonlinear and change character with the amplitude of deviations from trim. Consequently, as with the conclusions from the vertical flight-path control study reported in this paper, the potential for such problems to occur on a different tiltrotor, or indeed any unconventional rotorcraft configuration, requires extensive and specifically detailed exploration.

Such exploration should include piloted simulation trials to understand better the flight manoeuvres susceptible to such APCs, and how different control strategies influence the outcomes. The exploration space here is vast and methods for identifying APC signatures (e.g. Ref [2]) will need to be developed to assist in gaining insight into the physics of the couplings. This can lead to the creation of new handling qualities criteria related to the kind of adverse APCs discussed in this paper. In [25], an assessment of tiltrotor handling criteria related to lateral-directional control was reported, endorsing the attitude bandwidth metric as appropriate for tiltrotor aircraft performing tracking tasks. Response bandwidth and the associated phase-delay are considered critical for the assessment of an aircraft's susceptibility to PIO-type APCs; but [25] did not address HQ criteria related to the non-oscillatory APCs examined in this paper.

A necessary further step should involve the development of new approaches to pilot training, or more generally PVS training, since the V side of a semi-autonomous aircraft will also need to be sufficiently intelligent to learn to recognise and avoid adverse APCs and their consequences; and not to compete with the human pilot. The link between HQ metrics and criteria and pilot training can be reinforced in these developments. Then, there is the question of how to ensure pilots are equipped with a solid grounding in aeronautical science so that they understand the importance of recognition and corrective control strategies. In this paper, we only briefly address this topic, as follows.

4.0 APC aeronautical knowledge for pilots; risks and safety margins

Most, if not all, of the APCs experienced with prototype or operational aircraft have been explained, usually after the event, by dynamic analysis based on approximate solutions to the equations of motion. Even for situations of bewildering complexity referred to in [1], explanations based on how aeromechanical forces and moments interact to deplete the natural aerodynamic damping or stiffness and drive an aircraft unstable will form the foundation for understanding and setting within the compendium of aeronautical knowledge. Wilbur and Orville Wright understood this, as the extensive entries in their daily diaries reveal [22]. They experienced both non-oscillatory APCs described in this paper, on several occasions, sometimes resulting in a crash, but the low-speeds of flight, and resilient design of their gliders meant that they could quickly learn from their mistakes and develop safer control strategies and design changes, e.g. interlinking rudder and wing warp to reduce adverse-yaw. Their problem-solving skills, aeronautical knowledge and understanding grew with their manual flying skills; as it should be in the flight training of the modern-day pilot of course. A question arises as to the depth of aeronautical knowledge required by pilots so that they understand the risks and how to maintain adequate safety margins associated with APCs. Drawing on such understanding in practice depends on the pilot's alertness and spare capacity for cognitive processing.

During the first decade of aviation, pilots would typically devote close to 100% of their mental and physical effort to the manual flying task, and the only means of training was to fly the aircraft. Any kind of emergency, for example an encounter with bad weather or engine failure, significantly increased the risk of a crash. Nowadays, of course, things are different. In normal situations, a rotary or fixed-wing pilot might devote only 30% or less of their effort to the flying task, the other 70% or more on mission management, navigation, communications, system health monitoring and other duties. Skills for the flying task, the manual command and corrective control strategies for guidance and stabilisation (G&S) are developed through training to be instinctive; motion sensations forming the inputs in these natural

feedback loops. However, a pilot needs to be sufficiently engaged in the G&S control loops for such instinctive responses to be fully effective. It is well understood that increased control automation reduces this engagement as augmentation functions take over the pilot's role. For a tiltrotor aircraft, such augmentation has a multitude of forms; e.g. stability and guidance, flight envelope protection and structural load alleviation; Reference [5] discusses how these functions feature in the V-22 Osprey. An important PVS design challenge is then to ensure that these operate cooperatively, rather than competitively, with each other and with the pilot. An equally important training challenge is to ensure that the pilot understands their role in the cooperate-compete tension, and how to develop appropriate risk-mitigation strategies.

A pilot's technical aptitude and problem-solving skills to deal with unexpected behaviour and emergencies are clearly critical here. These are mostly honed during ground-based simulation training, and this is also where a pilot can learn to deal with APCs, i.e. be able to identify, diagnose and correct behaviour quickly enough to avoid departure or loss of control. The opportunity is taken in this paper to propose an approach to aeronautical knowledge capture and skill development for pilots, providing learning that endures. This is particularly germane to tiltrotor aircraft as they enter commercial service with a wide range of new operational capabilities. In [26], the first author described a problem-based-learning (PBL) module that featured as part of the final-year Master's programme in Aerospace Engineering with Pilot Studies at the University of Liverpool. The module was introduced within Liverpool's Active Learning agenda where the focus was on acquiring knowledge and skills through contextualised problem framing and problem solving. The approach should be familiar to pilots but the formalised framework of PBL, which includes deep reflections recorded within personal learning journals, reinforces the lasting value of the learning.

PBL exercises related to APCs could be embedded within normal training schedules addressing, for example:

a) Transformation of aeronautical knowledge currently found in pilot's handbooks into dynamic forms; specifically, impact on PVS stability and response rather than aircraft trim.

b) Demonstration of the impact of different closed-loop control strategies on stability; how weakly controlled dynamics can be driven unstable, e.g. loss of speed stability under flight-path control, loss of yaw stability under roll control.

c) For PIO-type APCs the solution often requires the pilot to back out of the control loop, but a PBL exercise could involve flying through the incipience in the controlled dynamic to demonstrate the impact.

d) Demonstration exercises at the edge of the flight envelope exploring so-called cliff-edge divergent APCs; these are usually caused by strongly nonlinear PVS characteristics, e.g. actuator rate limiting, augmentation function conflicts; the bewildering complexity at envelope edges referred to in [1].

Creating simulation-based PBL exercises around such problems raises the question, 'what are the necessary simulator fidelity requirements to ensure sufficient realism for training APC events?' This is closely linked to understanding the simulator requirements for training in, more general, rotorcraft loss-of-control in-flight (LOC-I, [27]) scenarios. As tiltrotors and other high-speed rotorcraft are developed and brought into service, the opportunity presents itself to address both the PBL outcomes and fidelity requirements in concert. A strong recommendation from the work presented in this paper is that this educational opportunity is wholeheartedly embraced by the industry to raise pilot awareness of the potential impact of adverse APCs on the safety of tiltrotor operations.

5.0 Conclusions and recommendations

In this paper, a theoretical approach for isolating the physics of a class of APCs has been presented. The approach has then been applied in two scenarios. The first relates to the classic problem of flight-path

management and speed instability during operations on the back side of the power curve. The second concerns strong control of roll attitude and the consequent loss of directional stability attributable to adverse-yaw effects. The study has been carried out using a FLIGHTLAB simulation model of the XV-15 research aircraft, described in detail in [5]. The study has focussed largely on non-oscillatory APCs that arise under strong control, with the weakly controlled dynamic driven unstable. From the results presented, the following conclusions are drawn and associated recommendations made.

5.1 APC analysis method for the PVS

The weakly coupled dynamic system partitioning can, with the underlying assumptions for mode separation and weak couplings satisfied, enable stability under strong control to be analysed to provide insight into the flight-physics of a class of APCs. Typically, weakly controlled dynamics are driven unstable by the couplings arising from strong control of a different dynamic. The changes in stability are typically reflected by the variations in effective stability derivatives that feature in the frequency and damping of the lower-order modal approximations.

To encourage greater understanding and wider practice of this form of APC analysis within the engineering community, it is recommended that the approach be included in flight dynamics and control modules at Masters-level Aerospace Engineering courses and short courses to Industry.

A principal recommendation from this study is that the theory should be applied in the HQ analyses for new rotorcraft configurations with coverage of practical manoeuvres throughout the flight envelope. Extensive investigations are required because, as described earlier in the paper, these low-frequency or non-oscillatory APCs are often hidden in the closed-loop dynamics, with subtle and insidious consequences.

5.2 Loss of stability from vertical flight-path constraint

A tiltrotor in H-mode displays similar behaviour to conventional helicopters under strong control of vertical flight path by cyclic. Below minimum-power speed, a surge mode features as the weakly controlled dynamic, driven unstable by a pilot or autopilot controlling flight path with cyclic. The stability boundary is reflected in the change of sign of the effective derivative X_{ueff}. In C-mode, the strong surge force from incidence perturbations (X_w) appears to protect the tiltrotor from the instability. In A-mode, the strong surge damping (X_u) from the proprotor governor system extends the surge mode stability into the back-side region.

The short-period mode is also driven unstable by proportional flight-path control, caused by the contribution of aircraft incidence to flight-path angle, increasing the risk of a PIO. Pilot lead, through inclusion of the flight-path rate change in the feedback loop provides effective stabilisation.

The analysis should be extended to explore the impact of flight-path control strategies on APCs throughout the flight envelope; the sensitivity to configuration could be explored on a baseline, like the FXV-15, but analysis needs to be applied to all new tiltrotor and other novel rotorcraft.

5.3 Loss of directional stability from roll attitude constraint

The effective weathercock stability (N_{veff}) reduces in the presence of adverse-yaw, leading to the risk of a yaw-sway divergent APC when the pilot controls roll attitude. For the FXV-15, the adverse-yaw was implemented through a coupling between aileron and differential-collective-pitch control. The level of pilot control gain required to destabilise the aircraft, changing the sign of N_{veff}, was shown to be a function of the ratio of natural dihedral to weathercock stability (L_v/N_v).

The analysis should be extended to explore the behaviour of this form of APC throughout the tiltrotor flight envelope for both A-mode and C-mode configurations. The behaviour will be considerably complicated when the pilot and augmentation functions are in competition; the analysis should be extended

into this nonlinear domain, to establish the safety margins for operation in the normal flight envelope of a tiltrotor.

5.4 Handling qualities standards

Existing handling qualities standards for fixed and rotary-wing aircraft do not fully address the kind of low-frequency, non-oscillatory APCs described in this paper. Requirements for flight on the back side of the power-curve are described in terms of trim characteristics, rather than closed-loop stability. Requirements for yaw stability in fixed-wing aircraft are described in terms of effective static stability; again, rather than closed-loop dynamic stability. The absence of established HQ standards for tiltrotor aircraft exacerbates this problem, but this issue was outside the scope of the present work, and our recommendation is more specific.

APC behaviour in tiltrotors should be examined within the context of the handing qualities standards to ensure that appropriate design criteria and test manoeuvres can be developed.

5.6 Aeronautical knowledge for pilots; risk and safety margins

Rotorcraft APC-related flight training is considered inadequate to assist pilots in the maintenance of adequate safety margins. An important factor here concerns the necessary simulator fidelity requirements for APC events and, more generally, loss of control situations. Current facilities are likely to have shortcomings, for both the flight-modelling and pilot-cueing systems. A problem-based learning approach to training pilots for APC events has been described; elements could be woven into the pilot-training programmes to draw out the important aeronautical knowledge required for pilots to fully understand the risks and associated safety margins throughout and beyond the edges of the normal flight envelope.

As tiltrotors and other novel rotorcraft enter commercial operations it is recommended that the PBL-approach described in this paper be included in basic and continuation pilot training programmes. Since much of the training will use flight simulators, it is recommended that an assessment of the fidelity requirements for such training be undertaken in concert with the development of the PBL material.

Acknowledgments. Material from this paper was presented by the first author at the International Workshop on Engineering for Rotorcraft Safety; April 7–9, 2021, Politecnico di Milano, as part of The European Commission H2020 Marie Skłodowska Curie Actions; MSCA-EJD, NITROS. The results presented in Figure 2 were drawn from the EPSRC grant Lifting Standards (EP/G002932/1). The use of the National Research Council Canada's Bell 412 ASRA facility in this research is gratefully acknowledged, along with the support from the NRC facility manager Bill Gubbels.

References

[1] McRuer, D.T., et al., *Understanding and Preventing Unfavourable Pilot-Vehicle Interactions*, National Academy Press, Washington, D.C., 1997.
[2] Mitchell, D.G. and David H.K. Identifying a pilot-induced oscillation signature: New techniques applied to old problems, *J. Guid. Control Dyn.*, 2008, **31**, (1), pp 215–224. DoI: https://doi.org/10.2514/1.31470.
[3] Pavel, M., Masarati, P., Gennarettic, M., Jump, M., Zaichike, L, Dang-Vu, B., Lu, L, Yilmaza, D., Quaranta, G., Ionitag, A. and Serafinic, J. Practices to identify and preclude adverse aircraft-and-rotorcraft-pilot couplings: A design perspective, *Prog. Aerosp. Sci.*, 2015, **76**, pp 55–89. doi: https://doi.org/10.1016/j.paerosci.2015.05.002.
[4] Pavel, M.D. and Padfield, G.D. Understanding the Peculiarities of Rotorcraft-Pilot Couplings, Proc. of the 64th Annual Forum of the American Helicopter Society, Montreal, Canada, May 2008.
[5] Padfield, G.D. Helicopter Flight Dynamics, Including a Treatment of Tiltrotor Aircraft, 3rd edition, Wiley, 2018, Chichester.
[6] Padfield, G.D. The Danger of Speed Instability Below Minimum Power; a Forgotten Problem? EASA Safety Workshop, 44th European Rotorcraft Forum, Delft, The Netherlands, 20th September 2018.
[7] Pinsker, W.J.G. Directional Stability in Flight with Bank Angle Constraint as a Condition Defining a Minimum Acceptable Value for N_v, RAE Technical Report 67 127, June 1967.
[8] Neumark, S. Problems of Longitudinal Stability Below Minimum Drag Speed, and Theory of Stability Under Constraint, Aeronautical Research Council ARC R&M. No. 2983, London HMSO, 1957
[9] Milne, R.D. and Padfield, G.D. The strongly controlled aircraft, *RAeS Aeronaut. Quart.*, 1971, **XXII**, (2), pp 146–168.

[10] anon, Descent Below Visual Glide-path and Impact with Seawall, Asiana Airlines Flight 214, Boeing 777-200ER, HL7742, San Francisco, California, July 6, 2013, NTSB accident report NTSB/AAR-14/01, PB2014-105984, June 2014.
[11] anon. Report on the Accident to AS332 L2 Super Puma helicopter, G-WNSB on Approach to Sumburgh Airport on 23 August 2013, AAIB Report 1/2016, Department for Transport, March 2016.
[12] Lu, L., Padfield, G.D. and Jump, M. Investigation of rotorcraft-pilot couplings under flight-path constraint below the minimum power speed, *Aeronaut. J.*, 2010, **114**, (1157). doi: 10.1017/S0001924000003882.
[13] Maisel, M.D., Giulianetti, D.J. and Dugan, D.C. The history of the XV-15 Tilt Rotor research aircraft; from concept to flight, NASA SP-2000-4517, NASA History Series, 2001
[14] Anon. "Certification Specifications and Acceptable Means of Compliance for Large Rotorcraft CS-29", EASA, Amendment 7, 15 July 2019.
[15] Duncan, W.J. *The Principles of the Control and Stability of Aircraft*, Cambridge University Press, 1952, Cambridge.
[16] McRuer, D.T., Graham, D. and Ashkenas, I. Aircraft Dynamics and Automatic Control, Princeton University Press, 1973 (page 457, Chapter 7.5).
[17] Du Val, R.W. and He, C. Validation of the FLIGHTLAB virtual engineering toolset, *Aeronaut. J.*, 2018, **122**, (1250), pp 519–555. doi: https://doi.org/10.1017/aer.2018.12.
[18] Padfield, G.D., Brookes, V. and Meyer, M. Progress in civil tilt rotor handling qualities, *J. Am. Helicopter Soc.*, 2006, **50**, (1), 50th Anniversary issue, pp 80–91.
[19] Cameron, N. and Padfield, G.D. Tilt rotor pitch/flight-path handling qualities, *J. Am. Helicopter Soc.*, 2010, **55**, (4), pp 1–13. doi: 10.4050/JAHS.55.042008
[20] anon. Flying Qualities of Piloted Aircraft, MIL-HDBK 1797, US Department of Defence, December 1997.
[21] anon. "ADS-33E-PRF, Handling Qualities Requirements for Military Rotorcraft", U.S. Army AMCOM, Redstone, AL, March 2000.
[22] McFarland, M.W. (editor), The Papers of Wilbur and Orville Wright, including the Chanute-Wright letters, Vol 1, 1899–1905, McGraw-Hill Book Company Inc., 1953, New York.
[23] Padfield, G.D. and Lawrence, B. The birth of flight control; with the Wright Brothers in 1902, *Aeronaut. J.*, 2003, **107**, (1078), pp 697–718. doi: https://doi.org/10.1017/S0001924000013464.
[24] Lawrence, B. and Padfield, G.D. Flight handling qualities of the Wright Flyer III, *AIAA J. Aircr.*, 2006, **43**, (5), pp 1307–1316. doi: https://doi.org/10.2514/6.2005-25.
[25] Meyer, M. and Padfield, G.D. First steps in the development of handling qualities criteria for a civil tilt rotor, *J. Am. Helicopter Soc.*, 2005, **50**, (1), pp 33–46
[26] Padfield, G.D. Flight handling qualities; a problem-based learning module for final year aerospace engineering students, *Aeronaut. J.*, 2006, **110**, (1104), pp 73–84. doi: 10.1017/S0001924000001020.
[27] White, M.D., Padfield, G.D., Lu, L. and Advani, S. Flight Training Device Fidelity Requirements to Address 'Rotorcraft Loss of Control Inflight'. Proceedings of the 75th Vertical Flight Society Forum, 13–16 May, Philadelphia, USA (2019)
[28] Milne, R.D. The analysis of weakly coupled dynamical systems, *Int. J. Control*, 1965, **2**, (2). doi: https://doi.org/10.1080/00207176508905535.

Appendix A. Underlying Theory for Analysing the Stability of Aircraft under Constraint

Small-perturbation dynamic motions of an aircraft can be described in the form of n, coupled, ordinary differential equations. This n-state system has n natural modes described by their eigenvalues and eigenvectors. For the case when the natural modes are widely separated, in terms of their eigenvalue location on the complex plane and the state-content of their eigenvectors, a useful approximation can be derived that effectively partitions the system into a collection of weakly coupled subsystems. The technique can be illustrated by considering the system partitioned into two levels, with states $\mathbf{x}_1$ and $\mathbf{x}_2$ (dimensions ℓ and m) such that $n = \ell + m$

$$\begin{bmatrix} \dot{\mathbf{x}}_1 \\ \hdashline \dot{\mathbf{x}}_2 \end{bmatrix} - \left[\begin{array}{c:c} \mathbf{A}_{11} & \mathbf{A}_{12} \\ \hdashline \mathbf{A}_{21} & \mathbf{A}_{22} \end{array}\right] \begin{bmatrix} \mathbf{x}_1 \\ \hdashline \mathbf{x}_2 \end{bmatrix} = \mathbf{0} \tag{A1}$$

Equation (A1) can be expanded into two first-order equations and their eigenvalues determined from the characteristic equations

$$f_1(\lambda) = |\lambda\mathbf{I} - \mathbf{A}_{11} - \mathbf{A}_{12}(\lambda\mathbf{I} - \mathbf{A}_{22})^{-1}\mathbf{A}_{21}| = 0 \tag{A2}$$

$$f_2(\lambda) = |\lambda\mathbf{I} - \mathbf{A}_{22} - \mathbf{A}_{21}(\lambda\mathbf{I} - \mathbf{A}_{11})^{-1}\mathbf{A}_{12}| = 0 \tag{A3}$$

We assume that the eigenvalues of the subsystems $\mathbf{A}_{11}\{\lambda_1^{(1)}, \lambda_1^{(2)}, \ldots, \lambda_1^{(\ell)}\}$ and $\mathbf{A}_{22}\{\lambda_2^{(1)}, \lambda_2^{(2)}, \ldots, \lambda_2^{(m)}\}$ are widely separated in modulus. Specifically, the eigenvalues of $\mathbf{A}_{11}$ lie on the complex plane within a circle of radius $r(r = \max|\lambda_1^{(j)}|)$, and the eigenvalues of $\mathbf{A}_{22}$ lie without the circle of radius $R(R =$

$\min|\lambda_2^{(j)}|$). The theory of weakly coupled systems [28] posits that the solutions to the characteristic Equation (A2) can be approximated by the roots of the first $m+1$ terms and the solution to the characteristic Equation (A3) by the roots of the last $\ell+1$ terms, solved separately. This hypothesis is valid when two conditions are satisfied,

(i) the eigenvalues form two disjoint sets separated as described above, i.e.

$$\left[\frac{r}{R}\right] \ll 1 \tag{A4}$$

(ii) the coupling terms are small, such that if γ and δ are the maximum elements of the coupling matrices $\mathbf{A}_{12}$ and $\mathbf{A}_{21}$, then

$$\left[\frac{\ell r \delta}{R^2}\right] \ll 1 \tag{A5}$$

When these conditions are satisfied, the eigenvalues of the complete system can be approximated by the two polynomials

$$f_1(\lambda) = |\lambda\mathbf{I} - \mathbf{A}_{11} + \mathbf{A}_{12}\mathbf{A}_{22}^{-1}\mathbf{A}_{21}| = 0 \tag{A6}$$

$$f_2(\lambda) = |\lambda\mathbf{I} - \mathbf{A}_{22}| = 0 \tag{A7}$$

The larger eigenvalue set is thus approximated by the roots of $\mathbf{A}_{22}$, while the smaller roots are approximated by $\mathbf{A}_{11}$ augmented by the quasi-steady behaviour of the faster subsystem $\mathbf{A}_{22}$. In [5], examples are presented showing how the approximation theory can be used to derive first or second-order approximations to a helicopter's natural modes, revealing the important derivatives that contribute to, e.g. phugoid or Dutch roll damping. As demonstrated in this paper, the method is particularly effective at describing the way dynamics are separated by the action of strong control.

Appendix B. Stability and Control Derivatives and Control Gearings for the FXV-15

Table B1. *FXV-15 longitudinal stability and control derivatives*

	u	w	q	θ	B_l	η	X_b
H-mode; 55kts, $\gamma = 3.5$deg							
X	−0.042	−0.007	−0.735	−9.811	4.597	0.908	−0.104
Z	−0.128	−0.310	20.393	0.233	5.079	1.116	−0.121
M	0.024	−0.024	−1.062	0.000	−5.735	1.845	0.352
H-mode; 75kts, $\gamma = 3.5$deg							
X	−0.059	−0.012	0.939	−9.774	4.099	1.727	−0.025
Z	−0.145	−0.618	38.906	0.885	9.673	2.073	−0.210
M	0.014	−0.037	−1.474	0.000	−5.684	3.403	0.458

Table B1. *Continued.*

	u	w	q	θ	B_1	η	X_b
60deg nacelle; 95kts, $\gamma = 3.5$deg							
X	−0.096	0.143	−8.793	−9.737	−3.514	1.773	0.243
Z	−0.089	−0.544	43.453	−1.223	12.288	2.974	−0.176
M	0.046	−0.142	−1.366	0.000	−3.266	4.567	0.435
60deg nacelle; 105kts, $\gamma = 3.5$deg							
X	−0.142	0.208	−4.037	−9.814	−6.931	2.927	0.432
Z	−0.059	−0.780	54.278	0.006	16.507	4.495	−0.195
M	0.031	−0.102	−1.521	0.000	−2.068	6.893	0.566
A-mode; 135kts, $\gamma = 3.5$deg							
X	−0.196	0.073	−10.03	−9.780	−3.215	2.455	0.178
Z	−0.150	−0.839	65.556	−0.823	1.642	7.132	0.518
M	0.096	−0.346	−1.593	0.000	−2.641	11.356	0.825
A-mode; 180kts, $\gamma = 3.5$deg							
X	−0.200	−0.011	−2.949	−9.809	−1.619	5.407	0.393
Z	−0.165	−0.980	91.461	0.327	−2.162	13.555	0.984
M	0.051	−0.340	−2.217	0.000	−1.203	21.400	1.554

Table B2. *FXV-15 control gearings [5]*

Longitudinal stick to elevator $\left(\frac{\partial \delta_e}{\partial X_b}\right)$		4.16°/in
Nacelle Angle (deg)		
Ref [13]	FXV-15 [5]	$\left(\frac{\partial B_1}{\partial X_b}\right)$ (°/in)
0 (H-mode)	90 (H-mode)	2.100
30 (C-mode)	60 (C-mode)	1.810
90 (A-mode)	90 (A-mode)	0.000

Cite this article: Padfield GD. and Lu L. The potential impact of adverse aircraft-pilot couplings on the safety of tilt-rotor operations. *The Aeronautical Journal*, https://doi.org/10.1017/aer.2022.20